1

ENERGY TRANSFER AND ELECTRONIC ENERGY MIGRATION PROCESSES

LI-JUAN FAN AND WAYNE E. JONES JR.

1.1 INTRODUCTION

1.1.1 Foundations of Energy Transfer and Energy Migration

Photoinduced energy transfer and energy migration processes have been studied extensively in luminescent polymers for several decades and have applications in sensors, optics, and solar energy conversion [1–7]. Energy transfer refers to a photophysical process whereby the excitation energy of an excited luminophore (donor "D") moves to a chromophore (acceptor "A"). This process can occur by either

Photochemistry and Photophysics of Polymer Materials, Edited by Norman S. Allen

a nonradiative process or a radiative process and is typically thermodynamically spontaneous. Within a unimolecular system, including macromolecules and one-dimensional polymer systems, this process is called electronic energy migration. This can occur between identical molecular subunits where no thermodynamic gradient exists or between different structures resulting in an energy transfer gradient. Thus, energy migration is a specific class of energy transfer. Here, the term "energy transfer" will be used to refer to an interaction between two different species ("heterogeneous" transfer) while the term "energy migration" to refer to processes involving the same species ("homogeneous" transfer), unless otherwise noted.

Electronic excitation results in a quasiparticle, termed an "exciton" in a one-dimensional polymer system [8–11]. When an insulator or a semiconductor absorbs light, an electron from the valence band is excited into the conduction band, and the missing electron in the valence band leaves a hole behind. The exciton can be regarded as a bound state of the excited electron and hole. It is an electrically neutral, excited state of the molecule. An exciton is mobile in a homogeneous one-dimensional system resulting in "hopping" of the exciton state among identical particles with equal energy rather than localizing on one chromophore. Therefore, energy migration can also be called "exciton migration" or "exciton hopping." The energy of a migrating "exciton" is not dissipated during migration; however, the kinetic relaxation of the molecule to the ground state results in a natural lifetime unless the exciton interacts with a lower energy trap site.

There are two nonradiative energy transfer mechanisms that can be described: the Förster mechanism and the Dexter mechanism [8,10]. Both energy transfer mechanisms occur through a radiationless process. Förster energy transfer, also known as through-space or dipole–dipole energy transfer, involves the long-range coupling of the donor and acceptor dipoles. The resonance between the donor dipole moment and the acceptor dipole moment is facilitated by the presence of intervening solvent dipoles. According to Förster, this kind of energy transfer mechanism is mainly affected by three factors: (1) the spectral overlap between the absorption spectrum of the acceptor and the fluorescence spectrum of the donor; (2) the distance between donor and acceptor since both dipole–dipole interaction energy and resonance are distance dependent; and (3) the orientation of the dipoles of the donor and the acceptor molecules and the intervening medium. The Förster energy transfer is favored when donor and acceptor are rigidly held in good alignment, because resonance is maximized when the oscillating dipole of the excited donor and the transition dipole of the acceptor ground state are aligned. The energy transfer rate (k_{ET}) for the Förster mechanism is described by the following relationship:

$$k_{ET}(\text{Förster}) = k\frac{\kappa^2 k_D^0}{R_{DA}^6}J \tag{1.1}$$

where k is a constant determined by experimental conditions such as solvent index of refraction and concentration, κ^2 is related to the interaction between the oscillating donor dipole and the acceptor dipole, which depends on the square of the transition dipole moments for the donor and the acceptor and the orientation of the dipoles in

space, k_D^0 is the pure radiative rate of the donor, J is the spectral overlap integral, and R_{DA} is the distance between donor and acceptor.

Dexter energy transfer is known as through-bond energy transfer and takes place through a double electron exchange mechanism within the molecular orbitals of the donor and the acceptor. The electronic coupling leading to energy transfer requires significant orbital overlap. Therefore, close interaction between the excited donor and the acceptor ground state is necessary. The rate constant of Dexter energy transfer, k_{ET}(Dexter), is shown below:

$$k_{ET}(\text{Dexter}) = KJ\, e^{(-2R_{DA}/L)} \tag{1.2}$$

where R_{DA} is the distance between donor (D) and acceptor (A) relative to their van der Waals radii L, K is related to the specific orbital interactions, and J is the normalized spectral overlap integral. Thus, the Dexter transfer rate is affected by the spectral overlap and also the separation distance between D and A.

The rates of the Förster energy transfer and Dexter energy transfer depend on the separation distance between the donor and the acceptor, shown qualitatively in Fig. 1.1. The former decreases as the inverse sixth power of the distance, whereas the latter falls off exponentially as the distance increases. Therefore, the Förster energy transfer is able to occur over very large distances, while Dexter energy transfer will give much greater rates at short distances and close contacts.

There is also a radiative energy transfer mechanism termed the "trivial" mechanism of energy transfer. It is accomplished through radiative deactivation of a luminophore donor and reabsorption of the emitted photon by a chromophoric acceptor. There is no direct interaction between the excited donor and the ground

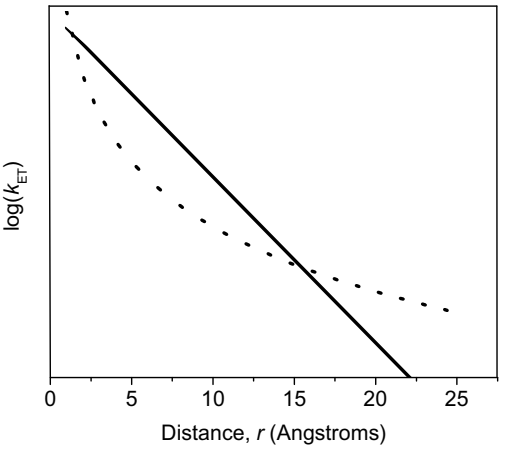

FIGURE 1.1 Plot of log(k_{ET}) versus distance r for both Dexter (solid line) and Förster (dotted line) energy transfer mechanisms, excluding any criterion other than distance. k_{ET} denotes the rate of energy transfer.

state of the acceptor. Thus, the "trivial" energy transfer is a two-step sequence as shown in Equations 1.3 and 1.4, where D^* and D denote the excited and ground states of the donor and A^* and A denote the excited and ground states of the acceptor.

$$D^* \rightarrow D + hv \tag{1.3}$$

$$hv + A \rightarrow A^* \tag{1.4}$$

The trivial mechanism is not very efficient given the statistical probability of direct emission and reabsorption. However, the efficiency of this kind of energy transfer can be maximized with high emission quantum yield of the donor, high concentration and high extinction coefficient of the acceptor, and strong overlap between the emission and absorption spectra. In most systems, the trivial process does not contribute significantly compared to the other two mechanisms.

1.1.2 Luminescent Polymer Systems

Excited-state processes in polymer materials strongly depend on their electronic and structural properties. There are several types of polymers that are capable of energy transfer and migration. A polymer with a saturated backbone and pendant chromophores such as naphthalene, anthracene, and commercial dyes can be described as type I polymer [11]. In some cases, the chromophore has also been incorporated as a component of the polymer backbone repeat unit or covalently linked to the polymer as a terminal end group. Typically, introduction of the chromophore is achieved through premodification of the monomers or postfunctionalization of the polymers.

The photophysics of type I polymers is very similar to that of the corresponding small-molecule substituent chromophores that they contain. The polymer can be described as an inert scaffold that restricts the movement and relative distance of the chromophores. As a result, the photophysics of these polymers can be strongly affected by the conformation of the polymer backbone and, to a lesser extent, by the aggregation of the polymers. The basic photophysics and energy migration processes of this type of fluorescent polymers have been studied extensively by Guillet and Webber over the past two decades and have been summarized elsewhere [1,11].

Another type of polymers involves conjugated backbones with extensive electronic coupling and has been classified as type II polymers. These so-called "molecular wire" conjugated polymers have received substantial and growing interest in recent years due to their potential wide application as light emitting diodes (LEDs), photovoltaics, and sensors [3,4,9]. Understanding energy transfer and migration in these polymer systems is critical to their success in these applications. An interesting subset of conjugated polymers is the group known as electrically conducting polymers first discovered in 1977 by MacDiarmid and Coworkers [12]. This Nobel Prize winning work has been described elsewhere and is beyond the scope of this review [13]. Here, focus will exclusively be on the fluorescent conjugated polymers that are typically semiconducting in nature.

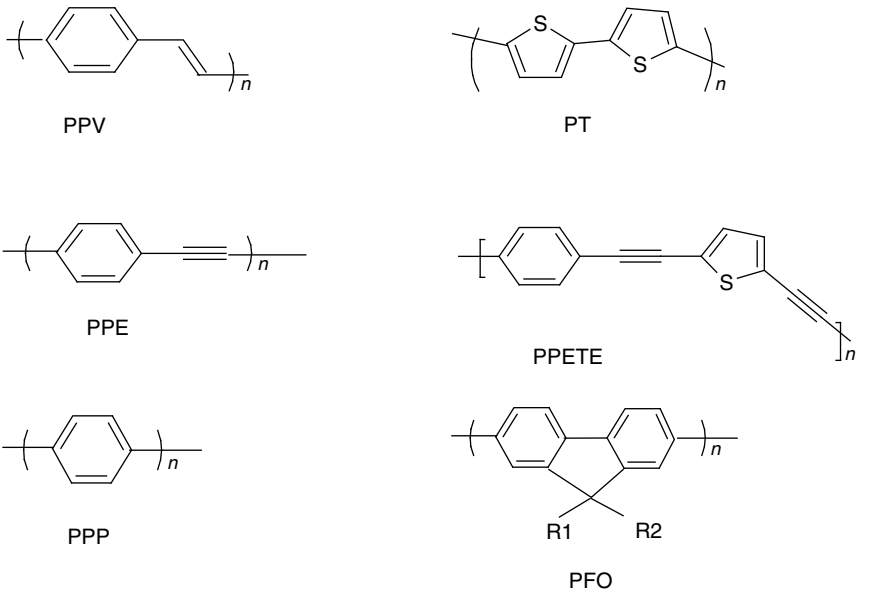

FIGURE 1.2 Basic structures of several fluorescent conjugated polymers.

There are two distinctive characteristics of conjugated polymer fluorophores relative to their small-molecule model compounds. The first is that the initial excited state formed by absorption of a photon is not a localized electron–hole pair. The excitation energy can be described as a delocalized *exciton* that spreads over several repeat units along the polymer backbone. The second characteristic is that the excitation energy can migrate along the polymer backbone. Some representative examples of conjugated polymer backbones are given in Fig. 1.2. They are poly (phenylene vinylene) (PPV), polythiophene (PT), poly[*p*-(phenylene ethynylene)] (PPE), poly[*p*-(phenyleneethylene)-*alt*-(thienyleneethynylene)] (PPETE), poly (*para*-phenylene) (PPP), and polyfluorenes (PFO).

Compared to type I fluorescent polymers, the conjugated polymer backbone is the active chromophore. The monomer units that make up the polymer might not be inherently fluorescent. The absorption and emission of photons involve electronic transitions between a ground-state singlet (S_0) and a excited-state singlet (typically S_1) as shown in Fig. 1.3. Radiative (k_r) and nonradiative (k_{nr}) transitions result in relaxation to the ground state and the observed kinetic lifetime τ of these systems is governed by the relationship

$$\tau = 1/(k_r + k_{nr}) \tag{1.5}$$

Introduction of transition metal elements might introduce significant spin–orbit coupling into the system that increases intersystem crossing, k_{isc}, and results in population of lower energy triplet states (T_1). The result is phosphorescence between the lowest energy triplet state and the ground-state singlet S_0.

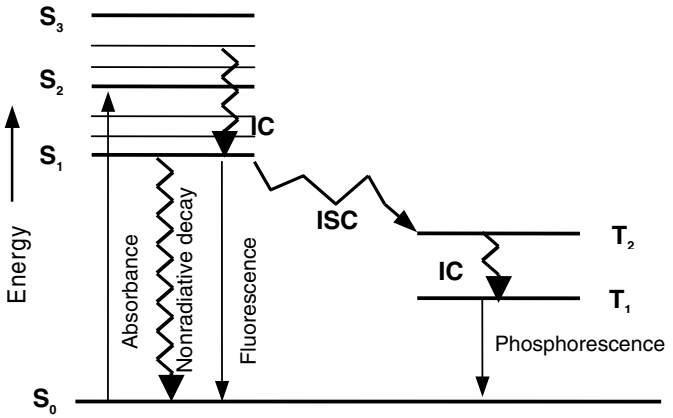

FIGURE 1.3 The Jablonski diagram. k_r, k_{nr}, and k_{isc} denote the rate constants of the deactivating processes from S_1; IC indicates the internal conversion process and ISC indicates the intersystem crossing process.

1.2 ENERGY TRANSFER AND MIGRATION PROCESSES IN CONJUGATED POLYMERS

1.2.1 Light Harvesting and Fluorescence Superquenching

Many applications of conjugated polymers take advantage of the facile energy migration that can occur through the extended π-system of the polymer backbone. The process can be represented using an electronic state diagram as shown in Figs. 1.4 and 1.5. The process of exciton migration has been described in the literature as following a random walk between energetically degenerate and equidistant chromophoric sites [9].

Here the natural lifetime of the exciton is not affected by the migration, although changes in polarization are evidence of the migration event. An exception to this

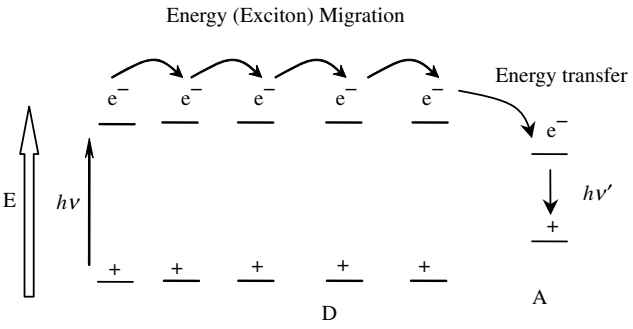

FIGURE 1.4 Illustration of the exciton (bound electron–hole pair) migration process in a conjugated polymer ending with a red-shift emission.

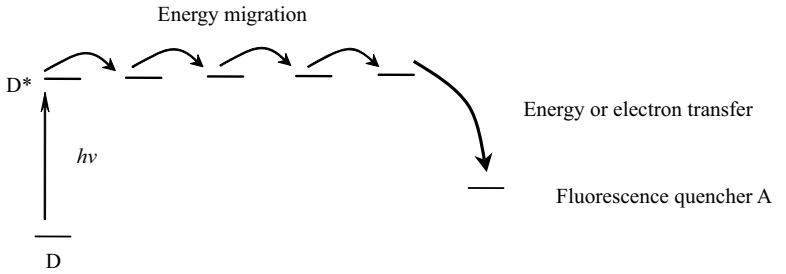

FIGURE 1.5 Illustration of energy migration from a donor state D^* to a fluorescence quenching acceptor site A.

would be when the exciton comes into proximity with an energy quenching site. This site could be a narrow-bandgap chromophore with emission at a long wavelength (Fig. 1.4) or a fluorescence quencher (Fig. 1.5). Two forms of energy transfer are involved in both situations: the energy migration among the identical excitonic sites of the polymer backbone (homotransfer) followed by energy transfer or electron transfer to a quenching acceptor (heterotransfer). Energy migration could occur over very large distances along the polymer chain depending upon the lifetime of the exciton and the relative loading of the acceptor.

The energy transfer situations depicted in Figs. 1.4 and 1.5 represent different models currently discussed in the literature. In the case of Fig. 1.4, the energy migration and transfer efficiency can be characterized by the emission ratio between the polymer backbone donor and the fluorescence from the acceptor group. This phenomenon has been called "light harvesting" since the conjugated polymer captures the incident light efficiently over the entire polymer and dumps the energy out at the lower energy trap site. This is the basis for solar harvesting in photosynthetic cells [1,3,14].

Superquenching of polymer fluorescence can be described based on Fig. 1.5. In this case, energy migration in the polymer and subsequent energy transfer or electron transfer to the acceptor is very efficient. Rapid exciton mobility combined with energy transfer to a trap site can result in million-fold amplification and the "superquenching" phenomenon in sensory system [6,9,15,16]. Superquenching has also been observed with gold nanoparticles in conjugated polymer systems further extending the scope of this phenomenon [17].

1.2.2 Intramolecular Versus Intermolecular Energy Migration

In recent years, there has been growing interest in understanding the energy migration processes that occur in conjugated polymer materials [3]. Many have found that the rate and efficiency of energy migration in conjugated polymers strongly depend on the conformation, aggregation, and electronic structure properties of the polymer. This dependence is due to the fact that energy migration processes can occur both intramolecularly and intermolecularly in different assemblies of the polymer materials.

In the case of a rigid-rod polymer in dilute solution, the system is free of any specific interaction between polymer chains or chain segments. In this case, the exciton usually follows a random walk along the polymer backbone, which is called "intramolecular energy migration process" [9,16]. When the polymer is in an aggregated state, the "intermolecular energy migration process" is the more dominant mechanism, although the intramolecular energy migration could still occur at a slower rate [18,19]. The aggregation state could be in several forms, such as specific interaction induced polymer aggregation in solution, spin-coating film, LB film, and self-assembled polymers onto the surface of a sphere [14,18–23]. Intramolecular energy migration takes place in one dimension, while the intermolecular energy migration takes places in two or three dimensions. Sometimes, polymer segments can fold back to form aggregation with another segment of the same polymer chain. The energy migration between these two segments is still classified as intermolecular here since it is more close to interchain migration as discussed in greater detail below.

Most conjugated polymers form aggregates at high concentration or in the solid state when the chains are in close contact. This aggregation tends to order the polymer chains, increasing p-conjugation and resulting in a red shift in the observed absorption and emission process. In some assemblies, well-packed conjugated chains preserve electronic independence and there is no observed interaction between the polymer chromophores. In other cases, the interaction between the conjugated segments results in the formation of new excited states such as excimers, exciplexes, and charge transfer species. When two adjacent polymer chromophores have π-electron interaction in the excited state but not in the ground state, the excited state is referred to as an excimer if the segments are identical or an exciplex if they are different. These aggregates are more common in the process of energy migration in condensed polymers.

1.2.3 Probing of Energy Migration in Different Conjugated Systems

There is considerable interest in understanding the mechanism and variables related to rate and efficiency for intramolecular and intermolecular energy migration in conjugated polymer systems. Many techniques, other than the room-temperature steady-state spectroscopy, have been used, such as single-molecule spectroscopy, time-resolved fluorescence spectroscopy, and low-temperature fluorescence and emission polarization spectroscopy. In addition, some specific conjugated polymers and assemblies have been designed to facilitate the study of isolated polymers or aggregated polymers with precise conformation or controlled migration. Some theoretical modeling and simulation have also been advanced by some groups for further understanding the experimental phenomena. Poly(arylene ethynylene) (PAE), PPV, and polyphenylene are the most discussed conjugated polymer systems in the literature and will be described in detail here as representative examples.

1.2.3.1 Poly(arylene ethynylene) Systems Energy migration processes in PAE have received great interest due to their relatively rigid structure, photophysical

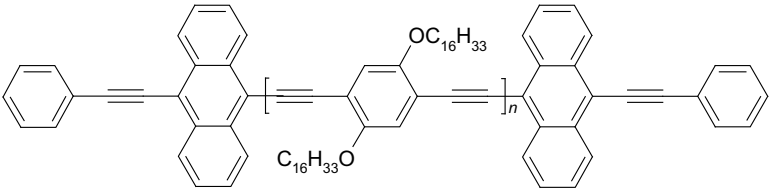

FIGURE 1.6 Structure of PPE endcapped with anthracene.

characteristics, and capability for facile long-range energy migration. Swager and coworkers have devoted considerable effort in this area, along with their outstanding research in the amplification of fluorescence-based chemosensory signal. One creative method for probing energy migration efficiency is to attach low-bandgap termini at the ends of a conjugated polymer chain. This was first demonstrated by Swager et al. in 1995 [24]. They synthesized the highly luminescent PPE polymer and incorporated anthracene into the backbone (Fig. 1.6). In this system, the polymer acted as an antenna that harvested the optical energy and transferred it to the low-energy anthracene group. The energy migration efficiency could be quantified by the emission ratio between anthracene and the polymer backbone. Figure 1.7 shows the absorption and emission spectra for this representative polymer. In this study, the absorption was a composite spectrum of the model PPE without the anthracene endcap and a model small-molecule anthracene chromophore. This suggested that the end group on the polymer produces very little perturbation in the polymer electronic structure. Interestingly, these low-energy termini were found to have a large effect on the emission behavior. Most emissions occurred in a band at 524 nm, which belonged to anthracene, while only a small amount (<5%) of emission at 478 nm was from the polymer backbone. This demonstrated that 95% of the excitation energy was

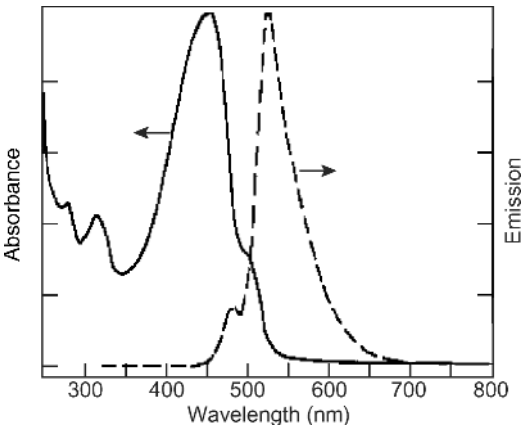

FIGURE 1.7 Absorption and emission spectra of the anthracene-endcapped PPE in dilute solution. For a detailed comparison among the spectra of the model polymer, anthracene, and this polymer, please see the original literature. (*Source*: Ref. [24].)

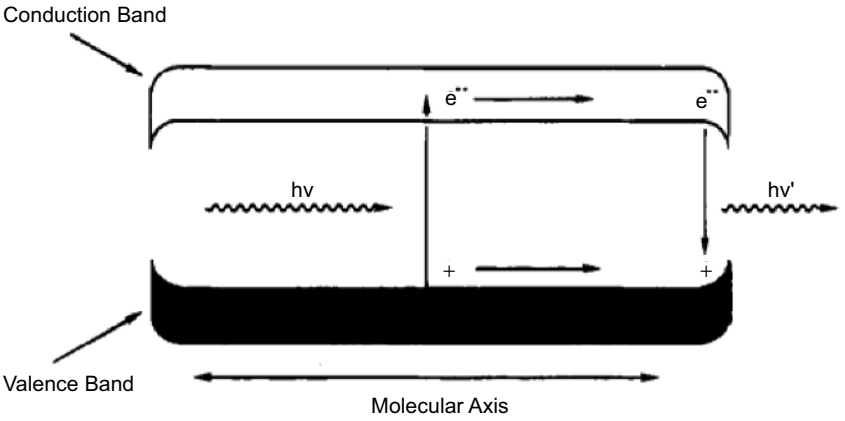

FIGURE 1.8 Schematic illustration of energy migration in a semiconductive molecular wire with a lower bandgap at the terminus. The exciton (the electron–hole pair) is initially generated by the photoexciton, migrates along the conjugated polymer backbone to the terminus, and then recombines with emitting fluorescence. (*Source*: Ref. [24].)

transferred to the end group and was attributed to facile energy migration in a semiconductive molecular wire with a decrease in the bandgap trap at the end (Fig. 1.8).

The molecular wire concept was first advanced in a chemosensory system by Swager and coworkers in 1995 [16,25]. In this case, energy migration could be classified as intramolecular, one-dimensional random walk since the photophysical study was carried out in dilute chloroform solutions. PPE is a rigid-rod polymer that suggested very little interaction between the polymer chains or segments at low concentrations. The one-dimensional energy migration along the polymer backbone can be described as involving through-bond Dexter energy transfer as a result.

One-dimensional random walks do not always provide for the most efficient energy migration. There are at least two reasons to explain the relatively sluggish one-dimensional energy migration in some systems. First, an excitation might retrace certain portions of the polymer backbone several times before quenching or relaxation. Second, the through-bond Dexter energy transfer process can be limited by orbital overlap as a result of chain defects, or conformational irregularities might exist in certain polymer backbones with more degrees of freedom.

To improve the efficiency of energy migration in chemosensory polymers, Swager et al. extended their interest in designing new conjugated polymers to assemblies capable of two- or three-dimensional random walks [14,18]. The idea was based on the consideration that increased dimensionality might decrease the probability of an excitation retracting a given segment of the polymer. In addition, multidimensional intermolecular energy transfer usually involves more facile Förster-type processes, which depend on the dipolar interaction between donor and acceptor [8,10].

The photophysics and energy transport properties of another PPE (Fig. 1.9) were investigated in highly aligned monolayer and multilayer Langmuir–Blodgett (LB) films as well as in the spin-coating film [18]. The cyclophane pendant group was

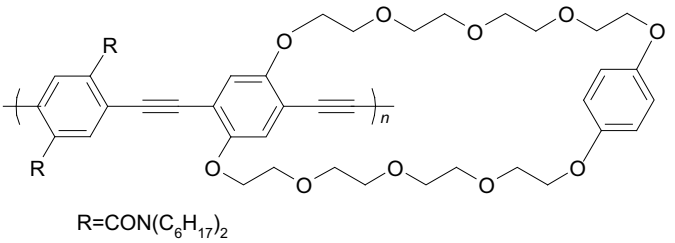

FIGURE 1.9 Structure of a PPE with cyclophane pendant group.

introduced in this case to prevent fluorescence self-quenching in the film due to intermolecular π-stacking between the fluorophores. Compared with fluid polymer solution, all the films displayed some degree of red shift. This was consistent with increased interaction (π-stacking) between the polymer backbones in the aggregated state (Fig. 1.10). The spectral profile in the case of the LB film showed a more limited change compared to the spin-cast film that was red shifted and exhibited a broadening in the spectra. A progression of red shifts in the LB film emission was observed with an increase in the number of layers, indicating more aggregation with increasing number of aligned layers in the films (Fig. 1.11).

Direct evidence of energy migration in the different films was found in polarized fluorescence emission studies. The fluorescence anisotropy indicated that intramolecular energy migration (with a Dexter hopping mechanism) existed in both the solution and spin-cast films. Further energy migration and transfer studies were

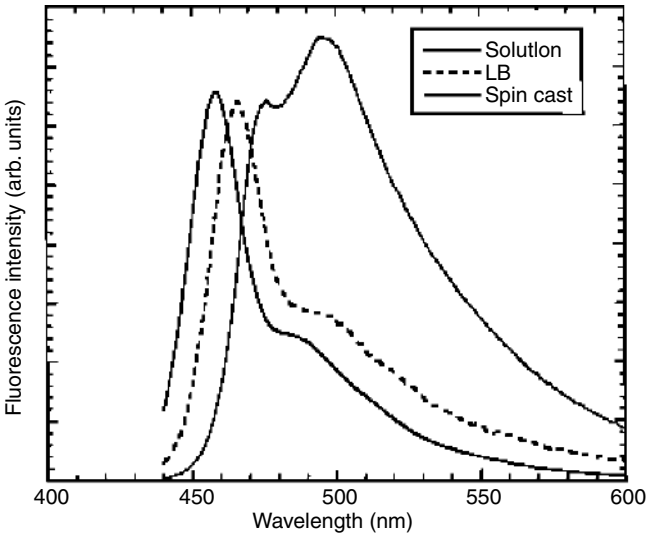

FIGURE 1.10 Comparison of the emission spectra for PPE with cyclophane pendant group (polymer in Fig. 1.9) in solution, as a highly aligned LB film (two layers) and as spin-cast from $CHCl_3$. The excitation wavelength was 420 nm. (*Source*: Ref. [18].)

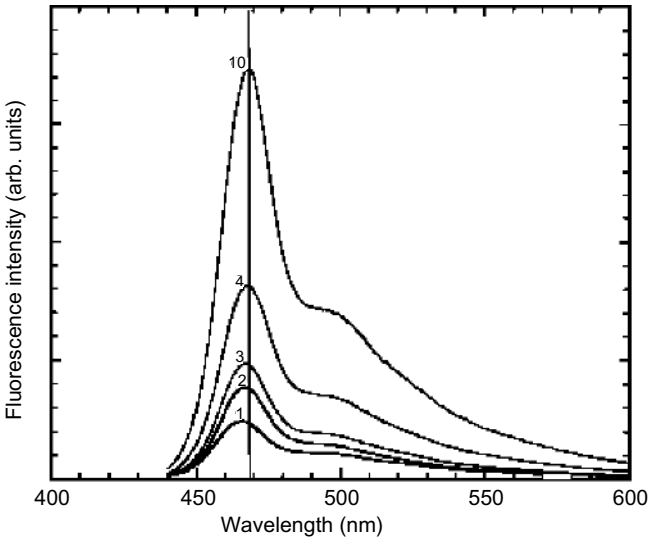

FIGURE 1.11 Emission spectra for LB films of the polymer in Fig. 1.9 containing 1, 2, 3, 5, and 10 aligned layers. The excitation wavelength was 420 nm. (*Source*: Ref. [18].)

carried out by using a luminescence trap Acridine Orange (AO) located on the polymer surface, which was prepared by dipping the LB film into the AO solution in methanol. As seen in Fig. 1.12, while selectively exciting the chromophoric polymer, the AO emission increases. This is accompanied by a decrease in the polymer

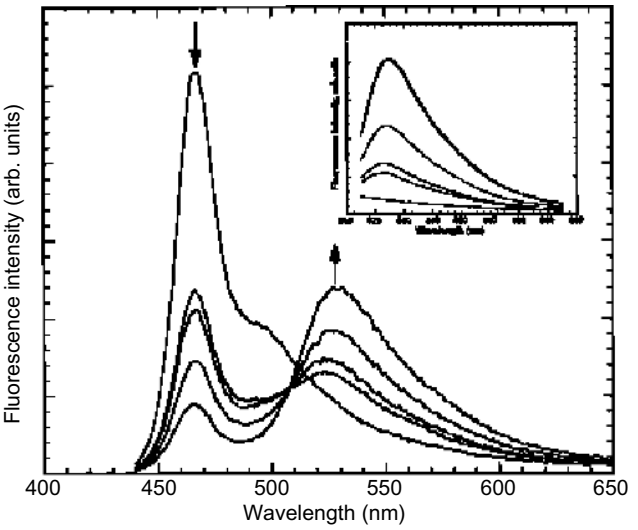

FIGURE 1.12 Emission ($\lambda_{ex} = 360$ nm) from a bilayer LB film of polymer in Fig. 1.9 treated with increasing concentrations (0, 8×10^{-8}, 1×10^{-7}, 3×10^{-7}, and 5×10^{-7} M) of AO in MeOH before dipping. The inset shows the emission spectra of the same films excited at 490 nm, where AO was selectively excited. (*Source*: Ref. [18].)

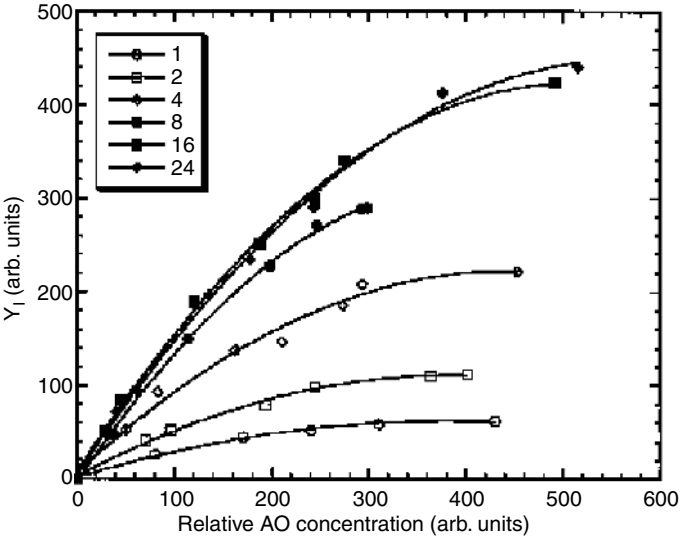

FIGURE 1.13 Summary of the AO fluorescence (excited at 360 nm, fluorescence detected at 525 nm) obtained from LB films of polymer in Fig. 1.9 containing different numbers of layers and concentrations of AO. (*Source*: Ref. [18].)

emission in the bilayer LB film. This phenomenon is consistent with that depicted in Fig. 1.4. The AO fluorescence intensity plotted against the relative trap concentration for LB films with different layers is shown in Fig. 1.13. The AO emission increases with an increase in the number of polymer layers until about 16 layers. The results indicate that energy migration takes place in a three-dimensional topology and that energy migration was very efficient. It was speculated that the energy migration saturates due to the diffusion length of the polymer exciton limiting access to all sites with higher numbers of layers.

Some theoretical work and computer modeling were also carried out in this system. The consistency between modeling and the experimental data suggested that both intralayer (in the film plane) and interlayer (normal to the LB film) energy migration have a very fast rate. The energy migration is dominated by a dipole–dipole (Förster-type) mechanism. This may be facilitated by the alignment of the rigid PPE molecules in the LB film.

Modifications to the secondary polymer structure can also be used to enhance intramolecular energy migration in dilute solution. By inducing the polymer chain into an extended conformation, there is increased π-conjugation and as a result energy migration [19,26]. For example, pentiptycene-incorporating PPE endcapped with 10-(phenylethynyl)anthracenyl has been synthesized by the Swager group (Fig. 1.14) [19]. The endcap was used as the energy trap in this case. The strategy was to introduce rigid and bulky tetra-*tert*-butylpentiptycene units in the backbone. This serves to limit the interchain interactions and at the same time makes the polymers more soluble. In addition, this bulky moiety has a substantial "internal free volume," which facilitates the polymer's alignment in nematic liquid crystalline (LC) media.

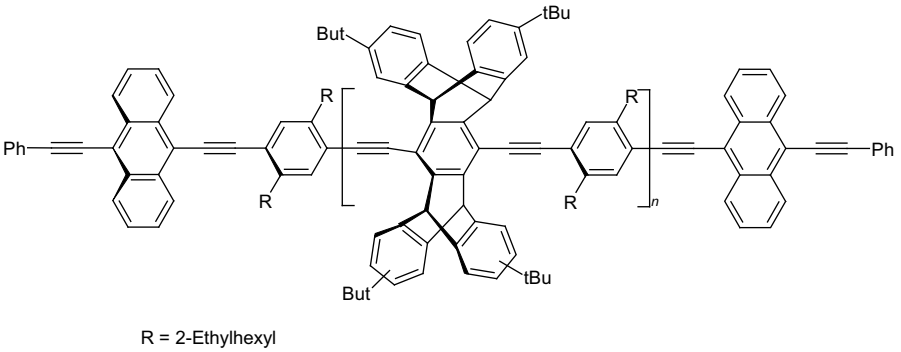

FIGURE 1.14 Structure of pentiptycene-incorporating PPE endcapped with 10-(phenylethynyl)anthracenyl groups.

The absorption and emission spectra of the polymer in CH_2Cl_2 solution, film, and LC solution are shown in Fig. 1.15. The fluorescence spectra were selectively excited into the p-conjugation of the polymer. In dilute CH_2Cl_2 solution, the polymer has an intense peak that can be attributed to the polymer backbone in both absorption (around 377 nm) and emission (around 420 nm). There is also a much weaker peak belonging to the end group at about 466 nm in the absorption and 500 nm in the emission. The red shift in absorption and the strong emission from the end group suggest facile energy migration in the polymer film. More interestingly, emission from the end group increases dramatically in LC solution. Both energy transfer efficiency (up to 36%) and quantum yield (0.90) increase significantly, compared to those in CH_2Cl_2 solution (approximately 7% and 0.60, respectively).

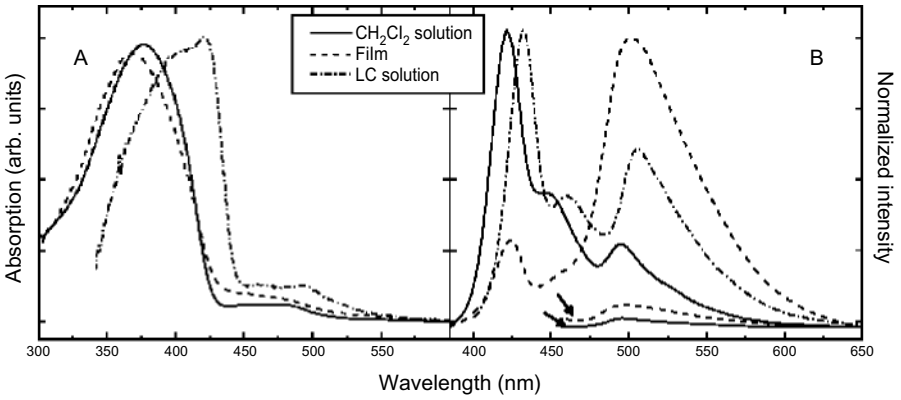

FIGURE 1.15 Normalized absorption (a) and emission (b) spectra of the polymer in Fig. 1.14. Emission spectra were acquired upon excitation at 370 nm and normalized according to the quantum yields. The lines marked with arrows correspond to the emission spectra obtained by direct excitation of the anthracenyl group at 450 nm. (*Source*: Ref. [19].)

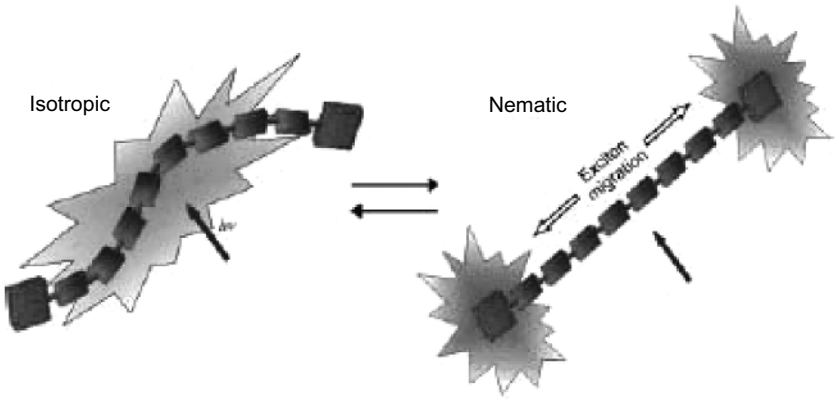

FIGURE 1.16 Simplified representation of the polymer shown in Fig. 1.14, in isotropic and LC solutions. (*Source*: Ref. [19].)

Enhancement in both energy transfer and total quantum yield was attributed to "the highly uniform alignment of the polymer chains and the increased electronic conjugation within the polymer backbone in the order LC phase" [19]. This was supported by further anisotropy experiments. The polymer exhibits much greater emission when excited parallel to the nematic LC direction than in the perpendicular direction. The rigidification and planarization of the polymer chains result in stronger electronic coupling along the polymer backbone, and thus increased conjugation (Fig. 1.16). It was concluded that intrachain Dexter energy migration was enhanced in LC solution compared with that in isotropic solution. The emission spectra in Fig. 1.17 supported the above arguments. The intramolecular Förster mechanism would not be expected to contribute to the enhanced energy migration since it increased the distance between the chromophores.

Energy migration has previously been shown to be involved in superquenching related to fluorescent conjugated polymer chemosensors. In this context, the role of different pendant groups and their structural spacing on energy migration has been studied by Jones and coworkers [15,27–30]. Energy transfer and migration in the PPETE system were studied extensively in dilute THF solution (Fig. 1.18). The study of the ttp-PPETE system involved energy migration leading to energy transfer at trap sites where transition metal cations were detected along the polymer backbone.

Stern–Volmer analysis provides a convenient method to study the binding event that leads to trapping of the energy migration. In this case, it was determined that a static quenching mechanism involving preexcitation binding of the metal cation was involved. This has also been observed in many other conjugated polymer chemosensory systems that involve energy migration [2]. Careful investigation showed that energy migration along the polymer backbone accounted for an observed upward curvature of the Stern–Volmer plot. A modified Stern–Volmer static quenching model was successfully applied to this system by incorporating an energy transfer term that takes into account different energy transfer mechanisms in the Stern–Volmer

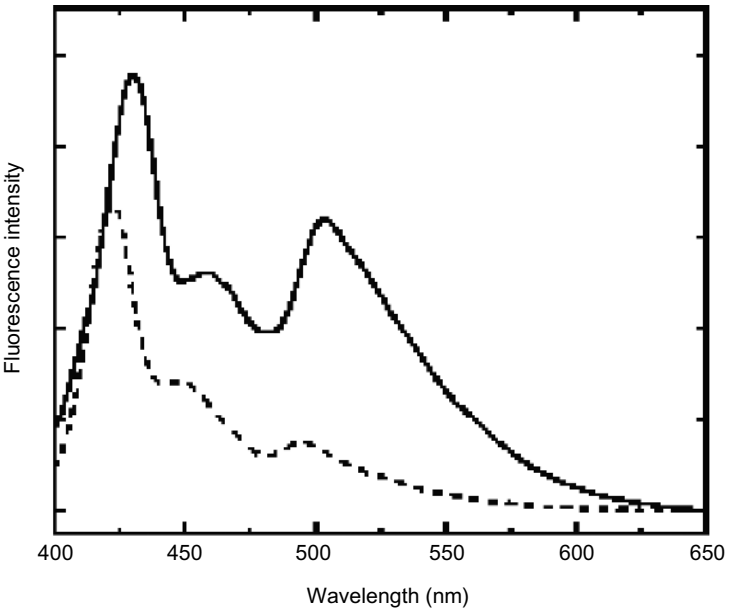

FIGURE 1.17 Fluorescence spectra of the polymer in Fig. 1.14 in the nematic LC phase at 25°C (solid line) and in the isotropic phase at 60°C (dashed line). (*Source*: Ref. [19].)

relationship. It was also demonstrated that the quenching mechanism, Förster or Dexter, was found to depend on the identity of the quencher analyte involved [27].

The (*x*% tmeda)-PPETE series are the polymers with PPETE as the backbone, having variable percent loadings of the *N*,*N*,*N*′-trimethylethylenediamino pendant group. The quantum yields were found to be directly related to the loading of the amino groups and can be modeled by a Stern–Volmer-type relationship. Photophysical studies related the total quenching efficiency to the inherent rate of photoinduced electron transfer from the amino group to the polymer backbone, the lifetime of the exciton, the rate of excitation energy migration along the polymer backbone, and the total loading of the receptor on the polymer. The amino group loading dependence of the fluorescence suggested that the energy migration along the polymer backbone

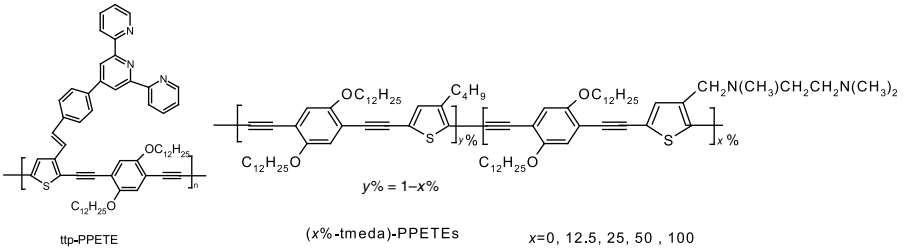

FIGURE 1.18 Structures of ttp-PPETE (left) and (*x*% tmeda)-PPETEs (right).

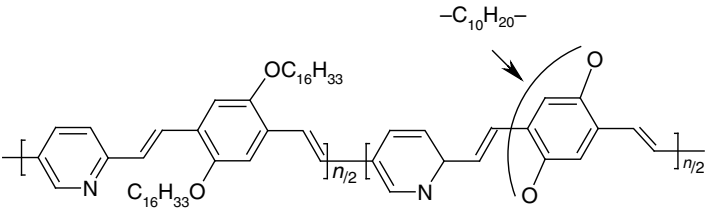

FIGURE 1.19 Structure of PPV-PPyV.

must be relatively slow. Cation titrations of this series of polymers showed no sensitivity enhancements with reduced receptor loading, which was consistent with the relatively sluggish energy migration along the polymer backbone [30].

1.2.3.2 Poly(phenylene vinylene) Systems PPV-type conjugated polymers have also received extensive interest during the past decade. The conformations of PPVs and their derivatives are more diverse than those of the PAEs since the PPVs have less rigid polymer backbone. Barbara and coworkers investigated the energy transfer processes of several PPV-conjugated polymers in a spin-cast film by single-molecule fluorescence spectroscopy (SMS) together with some other techniques [31–33]. Direct information about the individual molecules, such as energy transfer for the single polymer chain, can be obtained from SMS studies.

Barbara and coworkers reported on the copolymer poly(*p*-phenylene vinylene-*co*-*p*-pyridylene vinylene) (PPV-PPyV) (Fig. 1.19) embedded in polystyrene films [31]. The surprising single-step photobleaching kinetics and discrete jumps in single-molecule fluorescence intensity indicated that the conjugated polymer chain is a multichromophoric system. In other words, there were different absorbing and emitting species in a single conjugated polymer system. However, there was strong communication between these chromophores, which facilitate energy transfer to a localized fluorescence quenching polymer defect.

Poly[2-methoxy,5-(29-ethyl-hexyloxy)-*p*-phenylene vinylene] (MEH-PPV) (Fig. 1.20) is one of the most studied conjugated polymers in the literature. Barbara and coworkers used time-resolved single-molecule spectroscopy to investigate the energy transfer process on isolated single molecules of MEH-PPV [33]. Their experimental results suggested that the intramolecular electronic energy transfer converts the mobile excitons to trapped excitons that are located at one or more low-energy regions (energy trap) on a timescale shorter than the excited-state lifetime.

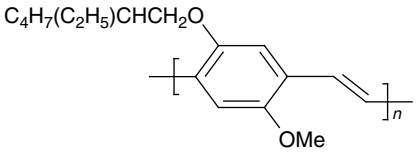

FIGURE 1.20 Structure of MEH-PPV.

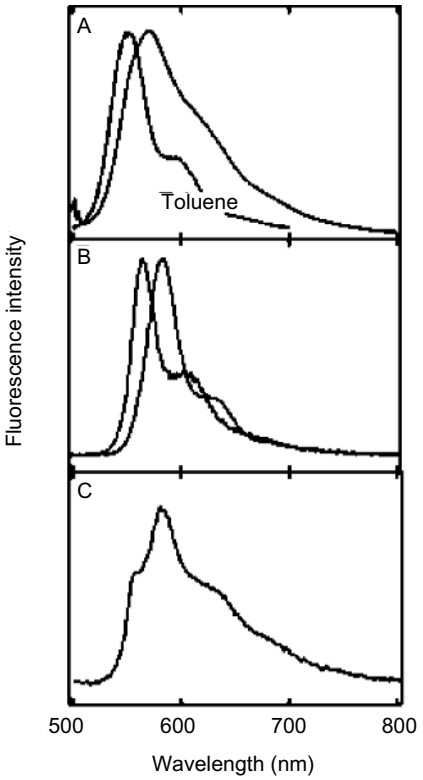

FIGURE 1.21 (a) The "ensemble" fluorescent spectrum of MEH-PPV in a pure liquid toluene solution (left peak) and in a polycarbonate matrix at ambient temperature (right peak). (b) Typical single-molecule spectra of MEH-PPV peaked at 560 and 580 nm. (c) A single molecule spectrum of MEH-PPV that has a "mixed" feature of both a 560-nm peak and a 580-nm peak. (*Source*: Ref. [33].)

Those energy traps, corresponding to the red shift peak in the SMS spectra (Fig. 1.21), come from the exciton interaction between nearby parallel oriented chromophores through the chain–chain contacts in the polymer "cylinder" conformation since different conformations exist in the polymer system (Fig. 1.22) [32]. There are some "funnels" such as the ordered-parallel-folded chain regions that favor rapid energy transfer due to the aligned transition dipole moments and short chromophore energy transfer distances. Further time-resolved emission transient indicated there are always several intermediate energy levels in the system, which also suggests that multiple energy transfer funnels exist. Thus, the whole system of the energy funnel could be envisaged as forming a "landscape for intramolecular electronic energy transfer" [33].

The picosecond time-resolved data (on a similar MEH-PPV single molecule) are also highly suggestive of rapid and efficient funneling of S_1 excitons to energy traps with oxygen quenchers [32]. The experimental result implies that a significant number

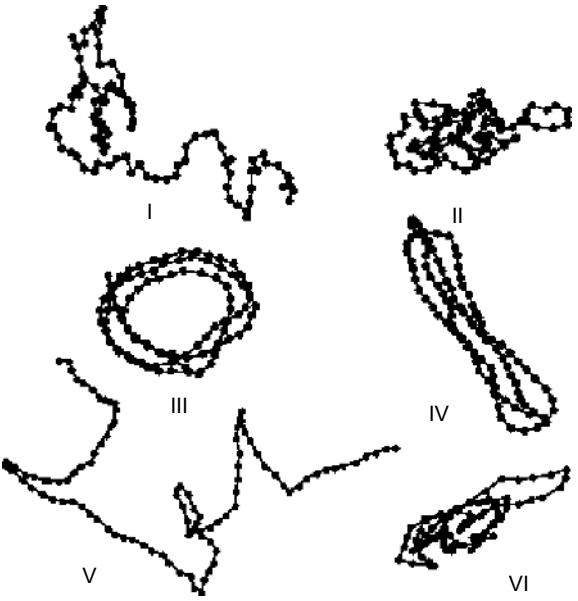

FIGURE 1.22 Typical conformations (I, random coil; II, molten globule; III, toroid; IV, rod; V, defect coil; VI, defect cylinder) of a 100-segment homopolymer generated by Monte Carlo simulations. (*Source*: Ref. [32].)

of the initially excited chromophores are associated with excitons that are transferred to the quencher in a timescale much less than 50 ps. However, measurements on a few of the single molecules reveal evidence of energy transfers (quenching) on a timescale as long as 100 ps. Therefore, slow and inefficient energy transfer still exists, perhaps in molecules with less conformational order. The intramolecular energy transfer is relatively slow. Fast energy migration in one molecule might take place among the different segments of the folded polymer chains. In addition, the nanosecond decay component associated with aggregation has not been observed in the time-resolved single-molecule fluorescence dynamics. This suggested that interchain interactions are required for MEH-PPV, as will be further confirmed by Schwartz and coworkers based on bulk spectroscopic data in the following example.

A more detailed investigation into the relative efficiencies of the interchain versus intrachain energy migration process in MEH-PPV was carried out by Schwartz and coworkers [34–37]. The ideal light harvesting or superquenching process should take place in a system where flow of energy can be controlled and directed to certain regions. To achieve the goal of controlling the energy flow, they constructed an artificial system consisting of a composite of conjugated polymer chains that have been aligned on the nanometer scale and encapsulated into the channels of a periodic mesoporous silica glass (Fig. 1.23) [34,35]. As shown in Fig. 1.23, the polymer chains within the channels are supposed to be well oriented and isolated from each other. However, the chain tails that extend out of the pores are randomly oriented and can be in contact with each other.

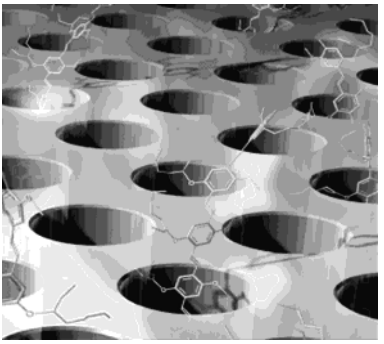

FIGURE 1.23 Schematic representation of single MEH-PPV chains embedded in the channels of an ordered mesoporous silica glass. Graphic courtesy of Daniel Schwartz, D.I.S.C. Corporation. (*Source*: Ref. [34].)

The steady-state and time-resolved luminescence were used to monitor energy transfer in the polymer/silica composites and to probe the fate of the emissive excitons created on the polymer chains after energy transfer (Figs. 1.24 and 1.25). The results showed that the aligned polymer chains inside the pores are isolated in a solution-like environment, and that the randomly oriented chains outside the pores have a degree of interchain contact similar to that in the film. In addition, the spectra indicated that excitons on conjugated polymer segments outside the pores, which are preferentially excited by the light polarized against the pore direction, migrate to lower energy segments inside the pores where they emit light that is red shifted and polarized along the pore direction.

Moreover, the role of interchain versus intrachain energy transfer in conjugated polymers was also separated in this specially designed system. The anisotropy data (Figs. 1.26 and 1.27) also suggest that although energy migration with a Förster mechanism between polymer chains (interchain energy migration) is fast, migration with the Dexter mechanism (intrachain energy migration) along a chain is unexpectedly slow. Correspondingly, the rapid anisotropy decay (Fig. 1.27) could be assigned to interchain energy transfer.

On the basis of the above experiments, the relative sequence of the interchain and intrachain migration in these composites could be described as follows. The interchain transfer takes place in a few picoseconds between the conjugated polymer segments outside the pores that are physically located within a Förster transfer radius. Once the energy has migrated sufficiently, there are no lower energy segments close enough for Förster transfer to occur, so interchain energy transfer ceases. Excitons can continue to migrate along the polymer backbone, from the coiled and nonaligned polymer segment with short conjugation length and high energy outside the pores to the straight and oriented polymer segments with longer conjugation length and lower energy, encapsulated within the channels, but as is evident from Fig. 1.26, they do so quite slowly, on a timescale of a few hundred picoseconds. Further investigation into this system led to the conclusion that the much slower energy migration along the conjugated polymer chain by roughly two orders of magnitude compared to energy

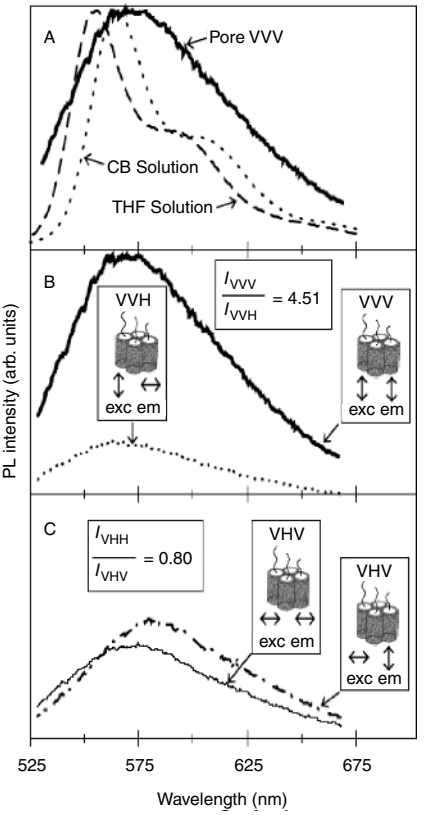

FIGURE 1.24 Emission spectra for MEH-PPV in different environments and under different excitation conditions. (a) Normalized steady-state PL spectra of MEH-PPV in chlorobenzene (CB) solution, THF solution, and the mesoporous silica composite with excitation and collection polarizations parallel to the pore direction (VVV). (b) PL of MEH-PPV in the nanostructured composite with excitation light polarized along the pore direction. The heavy solid curve [VVV, same as in (a)] shows emission collected polarized along the pore direction. The dotted curve (VVH) is for emission collected polarized perpendicular to the pore direction. (c) PL of MEH-PPV in the nanostructured composite with excitation light polarized perpendicular to the pore direction. The dot-dashed curve (VHV) shows emission collected polarized along the pore direction, and the thin solid curve is for emission collected polarized perpendicular to the pores (VHH). (*Source*: Ref. [35].)

transfer between conjugated polymer chains has important implications for devices based on these materials [35].

Structural variation through careful synthetic manipulation, such as controlling the conjugated length of the polymer chromophore or varying the chromophore distance on the polymer backbone, was an alternative way to investigate the energy transfer process. Padmanaban and Ramakrishnan prepared soluble MEH-PPV with a statistical control of the conjugation length over a very wide range by selective elimination

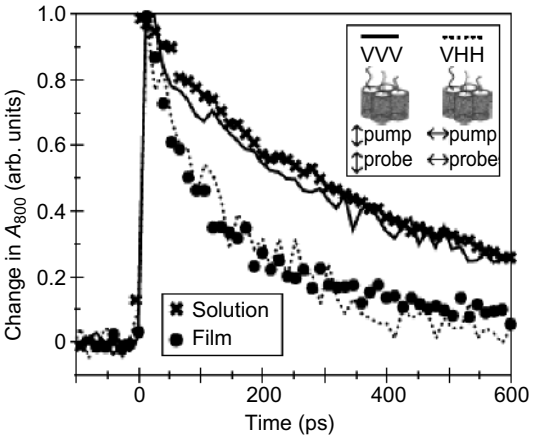

FIGURE 1.25 Ultrafast transient absorption dynamics of MEH-PPV in different environments probed at 800 nm after excitation at 490 nm, normalized to the same intensity at time 0. All four curves (solution, film, VVV, and VHH) were taken under identical excitation conditions. (*Source*: Ref. [35].)

of acetate groups in the sulfone-sulfoxide precursor while leaving the methoxy group unaffected (Fig. 1.28) [38].

The red shift in the absorption and emission with increasing statistic conjugation length was consistent with the initial expectation for the MEH-PPV-*x*s in the solution

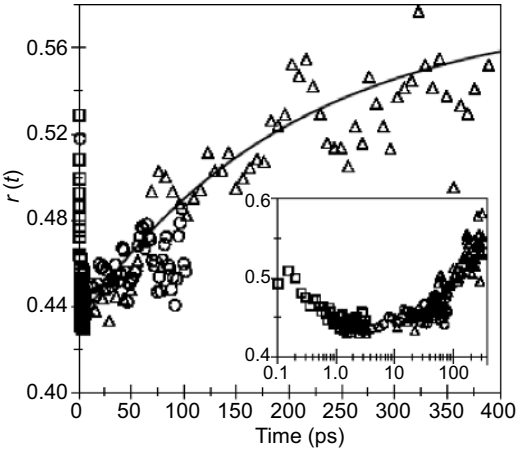

FIGURE 1.26 Ultrafast stimulated emission anisotropy of MEH-PPV in mesoporous silica glass with the excitation pulse polarization parallel to the pore direction (excited at 490 nm and probed at 590 nm). The solid curve in the figure is a 250-ps exponential rise and the different symbols represent scans taken with different amounts of time between points. □, 0.067 ps per point; ○, 1.67 ps per point; △, 6.67 ps per point. The inset shows the same data with a log scale for the time axis.

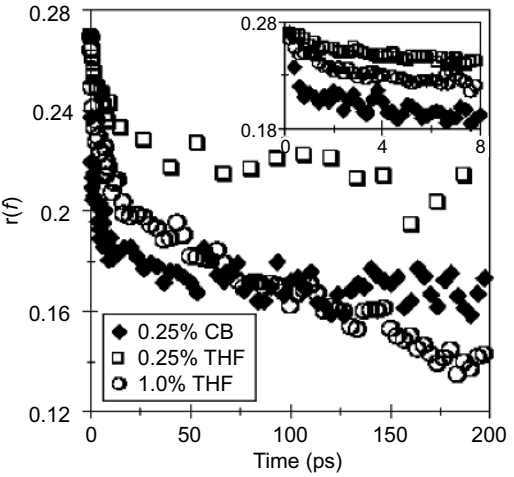

FIGURE 1.27 Ultrafast stimulated emission anisotropy of MEH-PPV in three different solution environments (excited at 490 nm and probed at 590 nm). The inset shows the early time dynamics on an expanded scale.

(Figs. 1.29 and 1.30). The fine structure of the spectra for the MEH-PPV-*x*s could be attributed to the existence of different lengths of conjugated segments. The control experiment for PPV oligomers with various conjugated lengths supported this deduction. Further comparison between the reconstructed and recorded spectra

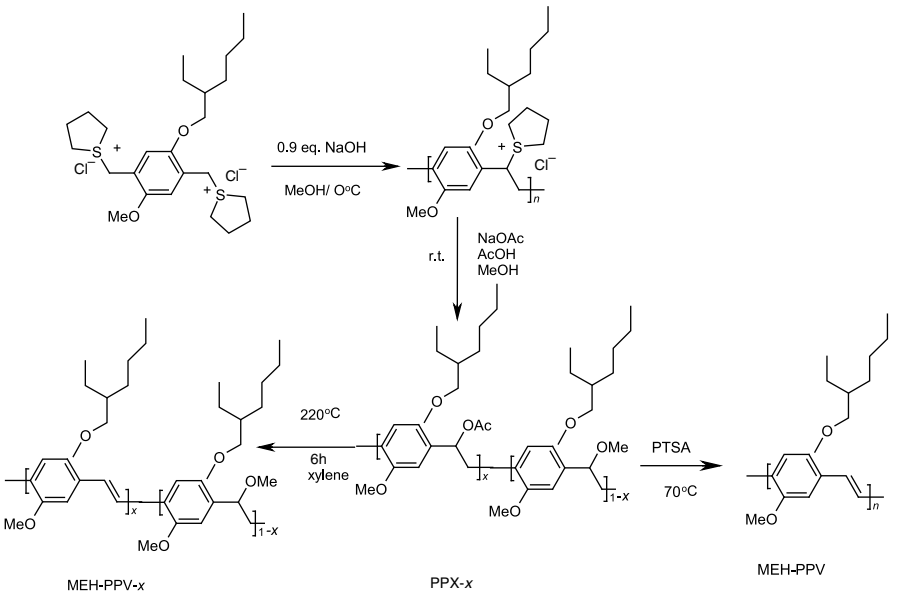

FIGURE 1.28 Synthesis of MEH-PPV-*x* and subsequent conversion to MEH-PPV-100.

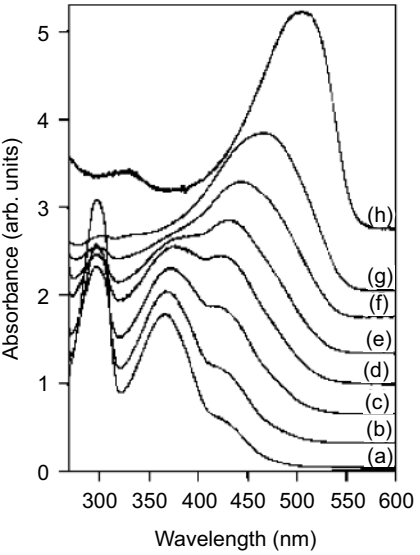

FIGURE 1.29 Normalized and Y-offset UV–visible absorption spectra of copolymers MEH-PPV-x: (a) $x = 10$; (b) $x = 20$; (c) $x = 30$; (d) $x = 45$; (e) $x = 55$; (f) $x = 69$; (g) $x = 85$; and (h) $x = 100$. (*Source*: Ref. [38].)

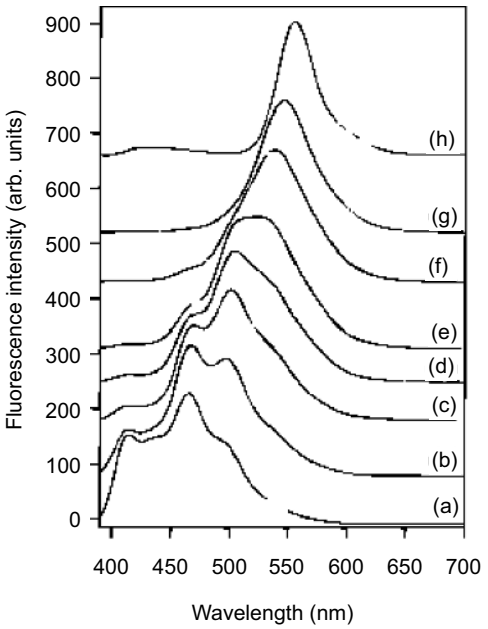

FIGURE 1.30 Normalized and Y-offset fluorescence spectra of copolymers MEH-PPV-x: (a) $x = 10$; (b) $x = 20$; (c) $x = 30$; (d) $x = 45$; (e) $x = 55$; (f) $x = 69$; (g) $x = 85$; and (h) $x = 100$. The concentration of the polymer is 10^{-6} M in CH_2Cl_2 and excited at 370 nm. (*Source*: Ref. [38].)

indicated the occurrence of intrachain energy transfer in the solution [reconstructed absorption spectra were obtained as follows: the individual probabilities of finding the various oligomer segments in each of the MEH-PPV-*x* samples were thus calculated and the absorption spectra of the OPV-*n* oligomers were factored (to reflect this expected oligomer concentrations) and summed up to generate the reconstructed absorption spectra]. In addition, in the case of the reconstructed spectra, no energy transfer is assumed to occur. The significant bathochromic shift of the spectra could be attributed to the chromophore aggregates. Devoid of the fine structure in the emission spectra of the MEH-PPV-*x* thin films indicated the presence of rapid excited energy transfer from short to longer conjugated segments and aggregates.

The extent of energy transfer was quantified by the fractional areas under the emission curves below and above 500 nm, which was calculated for both the reconstructed and the observed spectra (Fig. 1.31). The difference in the fractional areas between the observed and reconstructed spectra is a reflection of the extent of energy transfer that has occurred in the polymers. (For detailed calculation and discussion, please see the original reference.) The results show that intrachain energy migration still exists in dilute solution even when conjugated polymer chromophores were truncated to different conjugated lengths on the backbone. In addition, the extent of energy transfer increases as the average conjugation length increases since the probability of finding neighboring lower energy segments increases. However, the fluorescence quantum yields of MEH-PPV-*x* samples decrease with an increase in the extent of conjugation, which is contradictory to the model PPV oligomer. The authors attributed this phenomenon to the presence of a distribution of conjugation length within a single polymer chain that facilitates the energy transfer and lowers the emission [38].

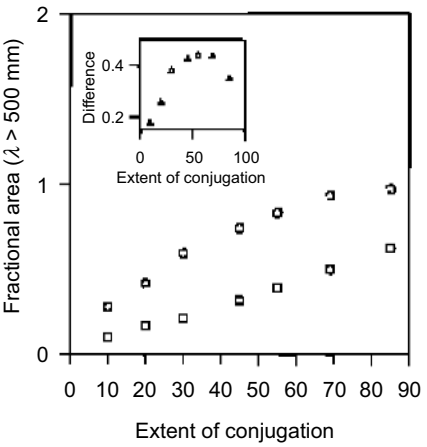

FIGURE 1.31 Plot of fractional area under the emission curve (CH_2Cl_2 solutions) for $\lambda > 500$ nm ($Area_{\lambda>500}/Area_{total}$) as a function of extent of conjugation "*x*". Open circles correspond to the recorded spectra, while open squares are for the reconstructed spectra. *Inset:* Variation of the difference of the fractional areas between the recorded and reconstructed spectra as a function of "*x*". (*Source*: Ref. [38].)

Peng et al. pointed out that energy transfer or energy migration has been extensively investigated in many artificial molecules and polymer systems [39]. However, energy transfer as a process in which excitation energy is released from one species to another has not been clearly stated in many occasions. They constructed a series of schematic diagrams of the situation in the polymer system where energy transfer might take place (Fig. 1.32) [39]. The energy transfer can be harvested and then transferred sequentially, directionally, and efficiently with multipigment array in photosynthesis (a). Energy transfer might take place between different pendent chromophores (b), or between the segments on the polymer backbone with the same chemical structures but different conjugation lengths (c). Since polymer could form aggregates with the other part of the same chain or from another chain, energy transfer could happen from the nonaggregated segments to the aggregates (d, e); Sometimes, the energy could be transferred from some pendant chromophore to the conjugated polymer backbone (f). Excited energy can also be transferred from the randomly directed conjugated polymer segments to the oriented parts (g). In some conjugated polymer systems, there exist aggregates with various extents of interactions between luminophores. Therefore, the energy could be transferred sequentially from the individual conjugated segments, through the loose aggregates, finally to the most aligned, compact aggregates (h).

Some of the energy transfer processes in Fig. 1.32 have been recognized, which were discussed in the above several paragraphs. However, the direct observation of the process itself in conjugated polymers, usually by time-resolved fluorescence spectroscopy, was rarely seen in the literature. The lack of the observation is possibly because energy migration or transfer is too rapid in fully conjugated polymers. In addition, it is

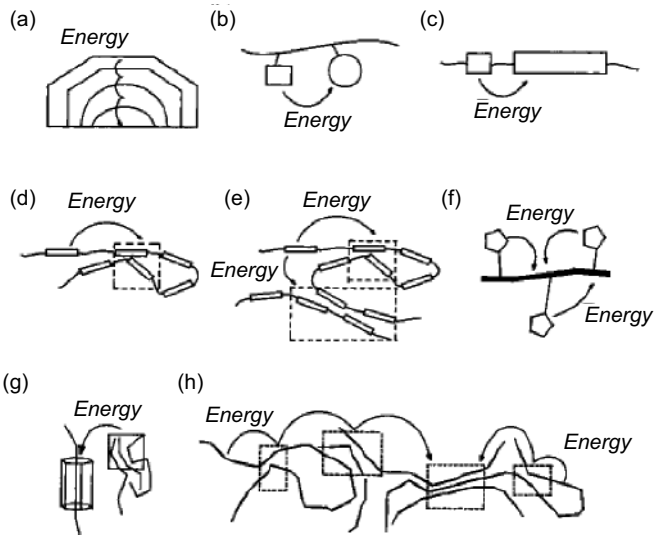

FIGURE 1.32 Schematic diagrams of the different environments for energy transfer, as discussed in the text. (*Source*: Ref. [39].)

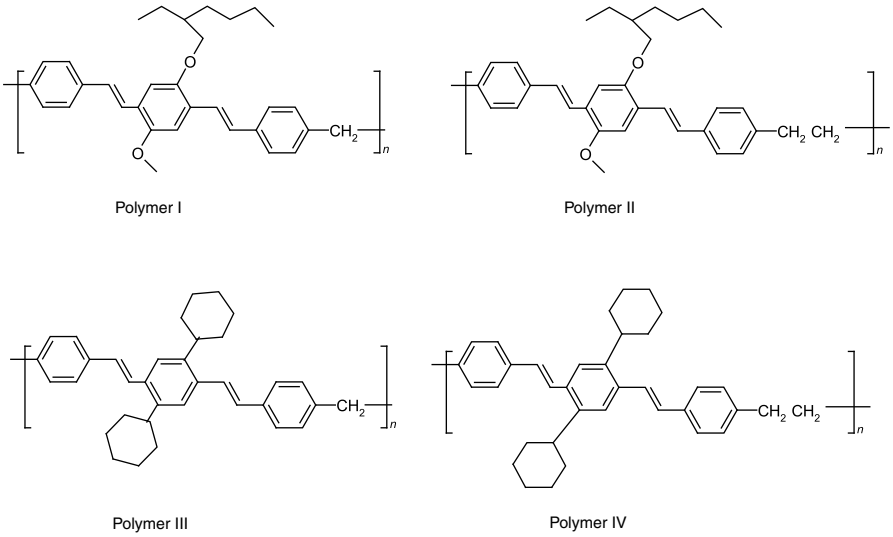

FIGURE 1.33 Structure of polydistyrylbenzene (PDSB) **I–IV**.

difficult to identify the energy transfer mechanism since it is complicated by a disordered environment. Peng et al. designed polymers with so specific structures to simplify the situation. They synthesized polymers of substituted distyrylbenzene (Fig. 1.33) with well-defined conjugation length as repeating units linked by methylene and ethylene linkages (polymers **I–IV** as shown below). The confusion in many other fully conjugated polymers, caused by the variation of conjugation lengths due to conformational distortion and tetrahedron defects, is excluded in these architectures. This series of the polymer could isolate the effects of interactions between individual luminophores (DSB units) on the photophysical properties and the effects of chemical structure on such interactions. In addition, the saturated spacer between the luminophores on the polymer backbone might slow down the energy transfer process to an extent observable by current available techniques.

They investigated the energy transfer process in the polymer chloroform solutions of various concentrations (0.01–10 mg/mL) and polymer films by UV–vis absorption and excitation, steady-state, and time-resolved photoluminescence spectroscopy. They found that the proximity between distyrylbenzene luminophores is critical to the interactions between luminophores and to the energy transfer processes. In concentrated solutions and solid films, aggregates exist besides the individual conjugated polymer chromophores. Different types of aggregates resulting from different extents of interactions, such as loose, compact, and the most aligned aggregates, between luminophores have been observed by photoluminescence.

They also directly observed the sequential energy transfer from individual DSB units to their aggregates and then from the loose aggregates to the relatively more compact aggregates by time-resolved fluorescence spectroscopy. This observation explained that the emission of the concentrated solutions and films of PDSBs **I–IV** is entirely or almost the aggregation emission in the steady-state spectroscopy.

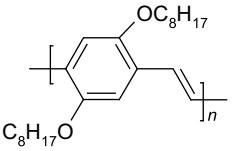

FIGURE 1.34 Structure of DOO-PPV.

However, such a sequential energy transfer process in fully conjugated polymers has never been directly observed at room temperature. The authors suggested that a similar process could take place in fully conjugated polymers with ultrafast dynamics due to the different lengths of the conjugated segments coming from the conformational distortion and tetrahedron defects, or the various extents of aggregation, although it is probably masked behind other photophysical processes [39].

The conformation of another PPV-type polymer, a long-chain 2,5-dioctyloxy-*p*-phenylene vinylene (DOO-PPV) polymer (Fig. 1.34), and photophysics and energy transfer were investigated by Chen and coworkers [40]. One important technique used by them for the study is the time-resolved fluorescence spectra, which was called fluorescence intensity–time trace in the original literature. This technique could provide valuable information on energy transfer as well as the number of emitters in the system studied. When the polymer system has only a few chromophores and luminophores, or very efficient energy transfer from many absorbing sites within the polymer to a few emitting sites, the trace would be dominated by one or two large steps. The appearance of many small steps or gradual changes in the trace would indicate that there are many insulated absorbing and emitting chromophores, lacking communication with each other.

Figure 1.35 presents a typical fluorescence time trace of an individual polymer. At short time intervals, this polymer exhibits multistep emission, while at a longer

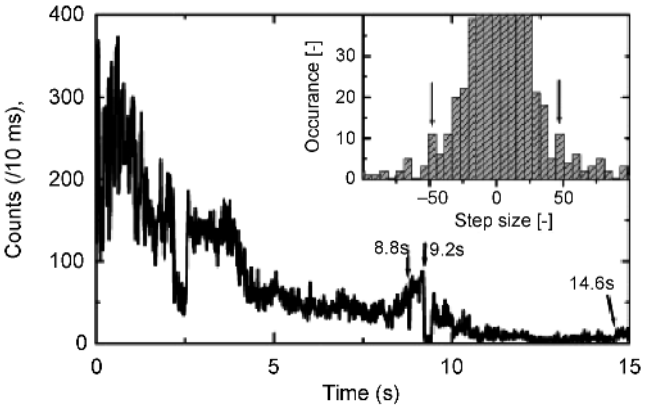

FIGURE 1.35 First 15 s of the fluorescence time trace of single long-chain DOO-PPV polymer under excitation with linearly polarized light recorded with 10 ms time resolution. The inset is a histogram of the change in intensity between each time interval. (*Source*: Ref. [40].)

timescale there is a slow smooth decay in emission intensity. There are several abrupt quantized intensity changes superimposed on small gradual changes in this trace. This phenomenon suggests that the polymer is composed of two types of regions. In the first region, which is responsible for the large jumps in intensity, three-dimensional energy transfers must be very efficient. Therefore, the excitation energy from many absorption sections was funneled to a few low-energy emission sites. The second region is responsible for the more gradual changes, indicating that many sections both absorb and emit. This could be attributed to the relatively inefficient one-dimensional energy transfer along the polymer backbone. For the polymer in Fig. 1.35, the first 3 s is characterized by both large abrupt fluctuations in emission and smaller changes in intensity on the order of the shot noise [40].

To further confirm the explanation made above for the fluorescence time trace, another new technique, the time-dependent modulation depth measurement, was performed on this polymer system. Observing the time dependence (or intensity dependence) of the modulation depth provides information on the relative orientation of the absorbing sections within the polymer. The results suggested that there is greater anisotropy in the orientation of absorption dipoles in the so-called "extended" region responsible for gradual changes, while the "core" region responsible for the abrupt changes has a slightly more isotropic arrangement of dipoles. Several conclusions can be made when combining the information from the fluorescence time traces and time-dependent modulation depth experiment. The first is that the energy transfer in the anisotropic extended region was not efficient (very likely the intrachain), leading to the existence of multiple absorbing and emitting sites. The second is the close packing in the relatively more isotropic "core" region, which allows efficient multidimensional energy migration from many absorbing to a few emitting sites. The results from the time-averaged and ensemble spectroscopic experiments on this polymer were consistent with the above conclusions [40].

Chen et al. synthesized another type of PPV, dialkoxy-substituted poly[phenylene vinylene]s (dROPPV 1/1, 0.2/1, and 0/1), consisting of two repeating units with different side chain lengths (methoxy and 3,7-dimethyloctyloxy) (see Fig. 1.36) [41].

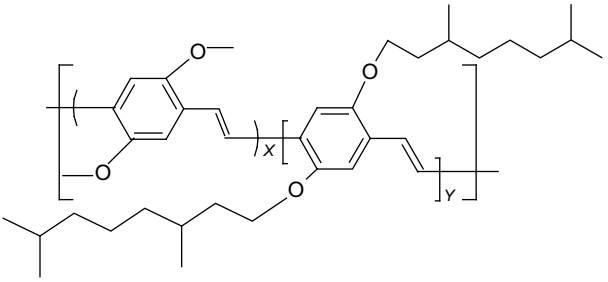

X/*Y*=1/1 dROPPV- 1/1
X/*Y*=1/5 dROPPV- 0.2/1
X/*Y*=0/1 dROPPV- 0/1

FIGURE 1.36 Structure of dROPPVs.

The control of the polymer conformation and aggregation state was facilitated by the fine-tuning of the copolymer composition, without altering the intrinsic properties of single polymer chains. In addition, these polymers can serve as "a model system to clarify roles of aggregates (the sites with ground-state interchain interactions) and the independent chain segments in the well-packed chains (the chain segments that are compactly packed without interaction) in the emission mechanism of conjugated polymers" [41].

The effect of the packing and aggregation of the polymer chain on the photophysics of the material was investigated by regular absorption and emission spectra, luminescence decay curve, and emission spectrum dynamics. These studies were carried out on the polymer chloroform solution as well as on the as-spin-coated films, annealed spin-coated films, as-casted films, and annealed cast films. The experimental results reveal that several kinds of polymer chain arrangement could exist in the polymer film (Fig. 1.37). One is the independent segments with random orientation in the loosely packed region. In the case of the well-packed region, sometimes the aggregates form, which are the ground-state species consisting of conjugated segments with an extension of π-system over one another. However, chains in the well-packed regions do not necessarily always form aggregates, especially for those rigid and orientated chain segments. These segments exhibit some photophysical characteristics of independent species with relatively long conjugation length. Therefore, as shown in Fig. 1.37, the energy transfer sequence could be from the independent segment in the loosely packed region to the independent segment with longer conjugated length in the well-packed chains and then to the aggregates [41].

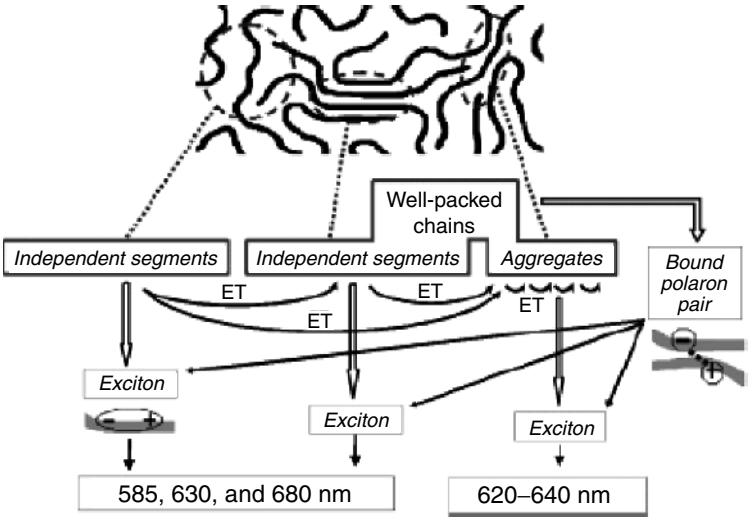

FIGURE 1.37 A proposed emission mechanism for the dROPPV polymers at the excitation of energy higher than the bandgap. (*Source*: Ref. [41].)

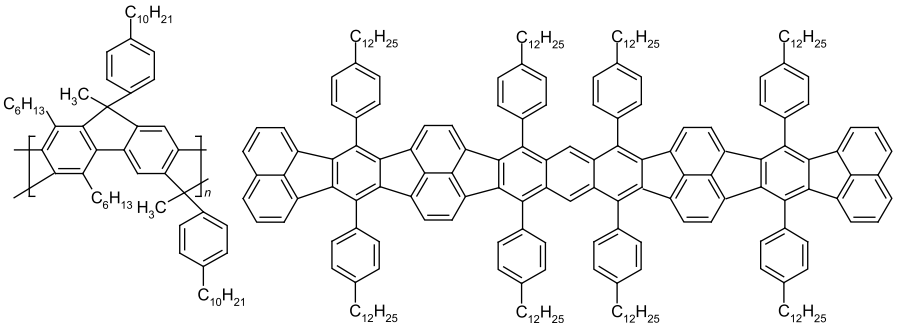

FIGURE 1.38 Chemical structure of m-LPPP (left) and RS19 (right).

1.2.3.3 Poly(para-phenylene) Another well-studied conjugated polymer is the ladder-type polymer PPP. The very extended and rigid molecular structure of this class of polymers avoids chain folding. In addition, the polymer luminophore aggregates are rarely found in these polymer materials due to their special structure. Therefore, the energy transfer process is relatively simpler than that in other conjugated polymers. Basically, it is well agreed that only intrachain energy migration along the polymer chain takes place in dilute solution, while the multidimensional interchain energy migration exists in the polymer films.

List et al. probed the energy migration EEM process in a methyl-substituted ladder-type poly(*para*-phenylene) (m-LPPP) through doping this material by small concentrations of a highly fluorescent p-conjugated macromolecule (RS19). The structures of the m-LPPP and RS19 are shown in Fig. 1.38 [42]. The experiments were carried out with various RS19 concentrations and under different temperatures. The experimental outcomes were discussed and modeled by Monte Carlo. Both the experimental and modeling results support the following picture for how the energy migration and energy transfer take place (Fig. 1.39). Energy transfer is always the sum of at least two processes in a system consisting of a polymer and a guest molecule, that is, the migration within the host, followed by a transfer to the guest.

The results from the experiment under various temperatures indicated that the first step is a temperature-dependent migration process of singlet excitons, which can be a

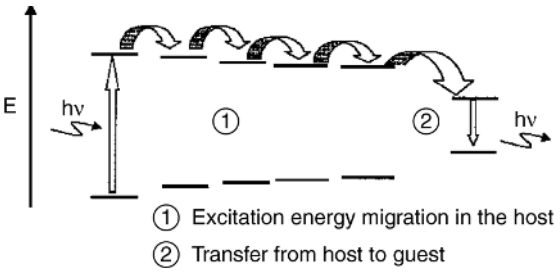

FIGURE 1.39 Schematic of the EEM process:. (*Source*: Ref. [42].)

Dexter- or a Coulomb-type energy transfer mechanism. However, the second step is a temperature-independent transfer, which could be attributed to a Förster dipole–dipole interaction type [42].

Müller et al. carried out low-temperature single-molecule spectroscopy studies on this rigid-rod ladder-type PPP in films without any other chromophore in the system [43]. The homogeneously broadened, strongly polarized emission from individual chromophore units on a single chain could be identified through this technique. Gated fluorescence spectroscopy found that the excitation energy transfer to the lowest energy chromophore is usually absent at low temperatures. The decrease in spectra overlap between the donor and acceptor units along the single rigid polymer chain accounts for the reduced energy transfer by lowering the temperature, considering the chromophoric spectral linewidth narrows with a decrease in the temperature [43].

Beljonne and coworkers explored the energy migration processes in a poly (indenofluorene) (PIF) endcapped with a perylene derivative (Fig. 1.40) by means of ultrafast spectroscopy with correlated quantum-chemical calculations [44,45]. The study of energy migration in dilute solution with a similar molecular design, a PPE-conjugated chain as the energy donor endcapped with anthracene as the acceptor, which was carried out by Swager et al., has been described in the previous paragraphs. In this system, the poly(indenofluorene) chains act as energy donors and the perylene derivatives as the acceptors. The contribution from the intrachain type or interchain type to the overall energy migration process was resolved by comparing the time-integrated luminescence with transient absorption spectra measured in solution and in films.

Basically, the slow intrachain energy migration was found to be dominating in the solution, on a timescale of 500 ps. However, the energy migration rate in a film turned out to be on a few tens of picoseconds scale, with one order of magnitude increase with respect to that in the solution. The high efficiency in films was attributed to the

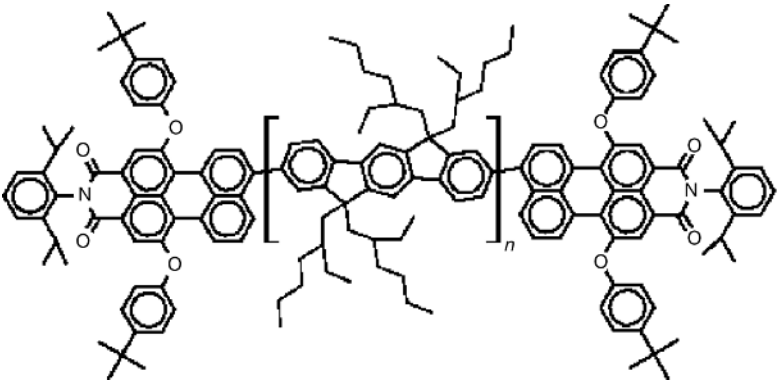

FIGURE 1.40 Molecular structure of R,*ö*-bis(*N*-(2,6-diisopropylphenyl)-1,6-bis-(4-*tert*-butylphenoxy)-3,4-dicarbonicacidimide-9-perylene-poly-2,8-(6,6,-12,12-tetraethylhexyl) indenofluorene (PEC-PIFTEH).

emergence of additional energy transfer channels due to the close contacts between adjacent chains. These findings were supported by computer modeling using the quantum-chemical calculations. The modeling was carried out on the basis that the whole transfer process was a two-step mechanism, which was also mentioned in the last example by List et al, that is, first a homonuclear energy migration among the conjugated polyfluorene chromophores and then a heteronuclear energy transfer to the perylene derivatives.

To rationalize the different dynamics observed in the solution and in the solid state, computer modeling was carried out step by step with gradually increasing level of sophistication [45]. The energy migration process in the solution was described as an intramolecular energy transfer process along the polymer chain, and only energy hopping to the nearest neighboring chromophores has been considered at first. Afterward, electronic couplings between the donor and acceptor chromophores, spectral overlaps between the donor emission and acceptor absorption, as well as the donor–acceptor relative orientation (which affects the electronic coupling) were taken into account. The energy transfer rates have been computed in the framework of an improved Förster model.

The homonuclear energy migration among the conjugated polyfluorene chromophores was found to be very slow due to weak electron coupling and small spectral overlaps. However, the heteromolecular energy transfer from an indenofluorene segment to an attached perylene derivative is calculated to be typically two orders of magnitude faster than that in the homonuclear process. The significant increase in the rates resulted from the higher electronic couplings and also more efficient donor–acceptor overlap in the second step of the energy transfer process as pointed out in Fig. 1.4. Thus, in situations where only intramolecular transfer takes place, the rate-determining step for energy transfer from the conjugated polymer to the end-capping perylene is the energy hopping process (Dexter energy transfer mechanism) along the conjugated main chains.

The modeling of the energy migration process in the film was a little more complicated. The intermolecular energy migration was possible since the two interacting poly(indenofluorene) chromophores can form different chains and in a cofacial arrangement. The electronic couplings and the corresponding homopolymer energy migration rates computed are always found to be larger than the corresponding intrachain values. In addition, the heteronuclear energy transfer between donor and acceptor was also found to be much faster when the perylene derivative was lying on top of the oligoindenofluorene segment compared to the situation when the donor and acceptor were lying on the same chain [45].

According to these results, it can be concluded that close contacts between molecules provide an efficient pathway for energy migration in conjugated materials as a result of increased donor–acceptor electronic couplings. That *interchain* exciton migration is faster than *intrachain* migration is consistent with the increase in transfer rate observed experimentally when going from solution to the solid state. The authors also pointed out that the rates of intrachain processes would increase significantly if the chains were perfectly conjugated and the excitations coupled coherently along the chains. Actually, the enhancement of energy migration by increasing the conjugated

polymer length has been demonstrated by Swager et al. through rigidifying the PPE polymer in a liquid crystal solvent.

The understanding of the long-range intrachain energy transfer process in conjugated polymer is very important for their application as light harvesting or superquenching materials. This process was modeled on the basis of the hopping rates calculated using the improved Förster model [45]. It was found that the transfer dynamics depends on the conjugated length and the distribution. Energy transfer is faster in polymers built from the short conjugated segments since the distance-dependent, site-to-site electronic coupling is larger in this situation. The modeling also showed that energy migration could experience more steps during the exciton lifetime with an increase in the total chain length, while the number of excitations effectively reaching the perylene group decreases.

Further theoretical analysis suggested a clear picture for the energy transfer and migration processes in this system. In a single polymer chain, the first step is the fast energy transfer from the closest indenofluorene units to the covalently attached perylene. Following this is the slow energy migration along the polymer backbone, from the relatively far conjugated polymer site to the closer site, finally reaching the perylene endcap. From the above discussion, it is obvious that the rate-limiting step for the overall excitation energy transfer process is the homonuclear energy migration along the polymer backbone. The simulated transient photoluminescence spectra agree well with the experimental results, supporting the above conclusions [45].

1.2.4 Summarizing the Characteristics of Energy Transfer and Energy Migration in Conjugated Polymers

There are still more excellent examples of the energy migration and energy transfer processes in the literature. They have not been included here due to the authors' limited reading and capability and the scope of this chapter. However, from the above discussion, it can be concluded that the energy migration and transfer processes in the conjugated polymers are very complicated.

First, even in the conjugated polymer materials with the same chemical structure, there are different absorbing and emitting species that affect the ground and the excitation energy and thus the energy transfer process. These absorbing and emitting species could be *independent polymer segments* with different conjugated length or *aggregates* with different extents of aggregation. Sometimes, the polymer segments remain independent even in some well-packed regions. The aforesaid complication, as discussed in great detail throughout this section, comes from the conformation variation in different environments, different structural defects formed during the synthesis, as well as some inherent characteristics of a specific type of polymer. Generally, the energy transfer takes place from the high-energy species to the low-energy species on the premise that all conditions are the same.

Second, the energy transfer taking place between chromophores of the same chemical structure was called "homonuclear energy transfer," while the term "heteronuclear energy transfer" was used to describe the process occurring between chromophores with different chemical structures. However, "energy transfer" is the

most common term sometimes used to describe all the processes mentioned above. In some cases, such as in most parts of this section, "energy migration" is used to refer to the process wherein the "homonuclear energy transfer" repeated many times, while "energy transfer" is used to refer to "heteronuclear energy transfer."

Third, the energy transfer mechanism could be the Dexter hopping mechanism, which relies more on the direct orbital overlap, and the Förster dipole–dipole energy transfer, which is more influenced by the relative orientations and the distance between the donors and acceptors. The Förster transfer is demonstrated to be much faster than Dexter transfer in the conjugated polymers.

Fourth, energy transfer or migration could take place intermolecularly or intramolecularly (between the different parts of the folded-back polymer chain classified as intermolecular transfer). It has been demonstrated experimentally and theoretically that the intermolecular energy migration is more efficient compared to the intramolecular one. Several reasons account for this difference. One is that intermolecular energy migration usually takes place via a Förster mechanism since the donor and acceptor belonging to different molecules could be in a cofacial arrangement in most cases, while the intramolecular one takes place via the Dexter mechanism since the donor and acceptor are neighboring on the same chain. Another reason is that intermolecular energy migration is always found in the close-packed region, especially in the film. Three-dimensional migration is possible and the "additional funnels" lead to more efficient migrations.

Finally, the energy migration could be "undirectional" or "directional." The unidirectional migration or "exciton random walk" usually takes place along the single polymer chain, where the conjugation length of the chromophore is considered to be identical, or different but statistically distributed. The intramolecular "random walk" leads to a slow energy migration since the exciton might revisit the sample many times. "Directional" migration takes place in specifically designed polymers constructed by chromophores with sequentially decreasing energy gap or in the polymer film or other forms where absorbing or emitting species of the same chemical structure but different energy gaps exist. The former requires more synthetic efforts, while the latter needs more control of the polymer conformation, aggregation, and packing. Obviously, the directional energy migration would be efficient and thus more useful in the application, which would be briefly discussed in the following section.

1.3 APPLICATIONS

The unique properties of the amplified fluorescent conjugated polymer due to their facile energy migration have been utilized in many applications, such as chemical sensors, biosensors, light emitting devices, and artificial light antennae. The application of conjugated polymer as sensors has been extensively reviewed by Swager et al. in 2000 and 2007 [2,5]. In their 2007 review, they have restricted their topic in sensor with fluorescence as the readout. The design of these kinds of sensors mostly took advantage of the energy migration in the polymer systems, which results in amplifying fluorescence signal output, and consequently enhanced sensitivity.

Some sensor designs make use of the superquenching phenomena (Fig. 1.5). Thus, the presence of the target analytes is indicated by the fluorescence intensity change. Other systems utilize the "light harvesting" properties (Figs. 1.5 and 1.39), and therefore, the presence of the analyte is signaled by the emission of another fluorophore.

As already detailed in Swager's reviews, some conjugated polymer sensory systems were in dilute solution where one-dimensional energy migration was predominant or in aggregation state where multidimensional energy migration was possible. The aggregation state could be achieved in concentrated solution, in films, coated on the spheres, and so on [14,18,20,21,25]. Sometimes, especially in the polyelectrolyte solution system, the analyte-induced aggregations provide additional sensitivity and selectivity [22,23,46–48]. The polyelectrolyte conjugated polymer system is especially useful in biosensors, which attracted many research efforts recently. In the case of DNA detection, the fluorescence resonance energy transfer (FRET) mechanism was used as the transduction pathway. The efficient light harvesting and emitting properties of the conjugated polymers make them excellent energy donors in these FRET-based sensing schemes. Bazan and coworkers have extensively explored these types of sensing systems [49–55]. These systems initially contain two major components: a water-soluble conjugated polymer cationic electrolyte and dye-labeled probe molecules. If the target DNA is added into the system, which has specific interaction with the probe molecules, the anionic DNA will bring the probe molecule close to the conjugated polymer, making the FRET between the polymer and the dye possible. Excitation of the polymer resulted in the emission of the dye as the signal output. Other systems were also developed with a similar mechanism.

Efficient energy migration and energy transfer were also used to tune the color emission of the fluorescence emitting devices such as polymer LEDs (PLEDs) [40,56–61]. Basically, some other emitting species such as dyes were covalently or noncovalently introduced into the conjugated polymer system. The efficient energy transfer from the polymer to the new fluorophore, or vice versa, causes the emission from the new fluorophores. Fine color tuning could be achieved by selecting different polymer and fluorophore matches, attaching the site (incorporated in the main chain, at the chain termini, or as side chain), or manipulating the morphology. In some cases, efficient white emission could be achieved through the incorporation of a low-bandgap green light emitting fluorophore and red light emitting moieties into the backbone of a blue light emitting bipolar polyfluorene copolymer. The energy transfer process, mostly the FRET process, was discussed more than migration.

Another promising application for conjugated polymer is its use in artificial antenna system. In these systems, the light harvesting was directed to an energy trap where many photoactivated processes, such as the photosynthesis, can take place. Because of their versatile physical and electronic properties as well as ease of synthetic control, porphyrins have been widely used as building blocks for such constructions. Up to now, the most studied system is dendritic or cyclic porphyrin arrays, which can direct all the absorbing lights into a core [62–68]. The goal of these

studies is to mimic the antenna effect in the biological system in the nature. This is also a direction for the conjugated polymers although few reports about other polymers besides porphyrins could be found in the literature [69].

REFERENCES

1. S.E. Webber, *Chem. Rev.* **1990**, *90*, 1469.
2. S.W. Thomas, G.D. Joly, and T.M. Swager, *Chem. Rev.* **2007**, *107*, 1339.
3. J.R. Terje and A. Skotheim, *Handbook of Conducting Polymers*, 3rd edition, CRC Press, 2007.
4. T.A.E. Skoheim, R.L. Elsenbaumer, and J.R. Reynolds (Eds.), *Handbook of Conducting Polymers*, 2nd edition, Marcel Dekker, New York, 1998.
5. D.T. McQuade, A.E. Pullen, and T.M. Swager, *Chem. Rev.* **2000**, *100*, 2537.
6. L.-J. Fan, Y. Zhang, C.B. Murphy, S.E. Angell, M.F.L. Parker, B.R. Flynn, and W.E. Jones Jr., *Coord. Chem. Rev.* **2009**, *253*, 410.
7. A.P. de Silva, H.Q.N. Gunaratne, T. Gunnlaugsson, A.J.M. Huxley, C.P. McCoy, J.T. Rademacher, and T.E. Rice, *Chem. Rev.* **1997**, *97*, 1515.
8. N.J. Turro, *Modern Molecular Photochemistry*, University Science Books, Sauslito, CA, 1991.
9. T.M. Swager, *Acc. Chem. Res.* **1998**, *31*, 201.
10. J.R. Lakowicz, *Principles of Fluorescence Spectroscopy*, Kluwer Academic/Plenum Publishers, New York, 1999.
11. J. Guillet, *Polymer Photophysics and Photochemistry*, Cambridge University Press, Cambridge, UK, 1985.
12. C.K. Chiang, C.R. Fincher, Y.W. Park, A.J. Heeger, H. Shirakawa, E.J. Louis, S.C. Gau, and A.G. MacDiarmid, *Phys. Rev. Lett.* **1977**, *39*, 1098.
13. A.J. Heeger, *Angew. Chem. Int. Ed.* **2001**, *40*, 2591.
14. D.T. McQuade, A.H. Hegedus, and T.M. Swager, *J. Am. Chem. Soc.* **2000**, *122*, 12389.
15. Y. Zhang, C.B. Murphy, and W.E. Jones, *Macromolecules* **2002**, *35*, 630.
16. Q. Zhou and T.M. Swager, *J. Am. Chem. Soc.* **1995**, *117*, 12593.
17. C. Fan, S. Wang, J.W. Hong, G.C. Bazan, K.W. Plaxco, and A.J. Heeger, *Proc. Natl. Acad. Sci. USA* **2003**, *100*, 6297.
18. I.A. Levitsky, J. Kim, and T.M. Swager, *J. Am. Chem. Soc.* **1999**, *121*, 1466.
19. E.E. Nesterov, Z. Zhu, and T.M. Swager, *J. Am. Chem. Soc.* **2005**, *127*, 10083.
20. J.H. Wosnick, J.H. Liao, and T.M. Swager, *Macromolecules* **2005**, *38*, 9287.
21. R. Deans, J. Kim, M.R. Machacek, and T.M. Swager, *J. Am. Chem. Soc.* **2000**, *122*, 8565.
22. C. Tan, E. Atas, J.G. Muller, M.R. Pinto, V.D. Kleiman, and K.S. Schanze, *J. Am. Chem. Soc.* **2004**, *126*, 13685.
23. J.G. Muller, E. Atas, C. Tan, K.S. Schanze, and V.D. Kleiman, *J. Am. Chem. Soc.* **2006**, *128*, 4007.
24. T.M. Swager, C.J. Gil, and M.S. Wrighton, *J. Phys. Chem.* **1995**, *99*, 4886.
25. Q. Zhou and T.M. Swager, *J. Am. Chem. Soc.* **1995**, *117*, 7017.
26. A. Rose, C.G. Lugmair, and T.M. Swager, *J. Am. Chem. Soc.* **2001**, *123*, 11298.

27. C.B. Murphy, Y. Zhang, T. Troxler, V. Ferry, J.J. Martin, and W.E. Jones, *J. Phys. Chem. B* **2004**, *108*, 1537.
28. L.J. Fan, Y. Zhang, and W.E. Jones, *Macromolecules* **2005**, *38*, 2844.
29. L.J. Fan and W.E. Jones, *J. Am. Chem. Soc.* **2006**, *128*, 6784.
30. L.J. Fan and W.E. Jones, *J. Phys. Chem. B* **2006**, *110*, 7777.
31. D.A. Vanden Bout, W.-T. Yip, D. Hu, D.-K. Fu, T.M. Swager, and P.F. Barbara, *Science* **1997**, *277*, 1074.
32. D. Hu, J. Yu, K. Wong, B. Bagchi, P.J. Rossky, and P.F. Barbara, *Nature* **2000**, *405*, 1030.
33. J. Yu, D. Hu, and P.F. Barbara, *Science* **2000**, *289*, 1327.
34. T.-Q. Nguyen, J. Wu, S.H. Tolbert, and B.J. Schwartz, *Adv. Mater.* **2001**, *13*, 609.
35. T.-Q. Nguyen, J. Wu, V. Doan, B.J. Schwartz, and S.H. Tolbert, *Science* **2000**, *288*, 652.
36. T.-Q. Nguyen, V.S. Doan, and J. Benjamin, *J. Chem. Phys.* **1999**, *110*, 4068.
37. B.J. Schwartz, *Annu. Rev. Phys. Chem.* **2003**, *54*, 141.
38. G. Padmanaban and S. Ramakrishnan, *J. Am. Chem. Soc.* **2000**, *122*, 2244.
39. K.-Y. Peng, S.-A. Chen, and W.-S. Fann, *J. Am. Chem. Soc.* **2001**, *123*, 11388.
40. W.-Y. Sun, S.-C. Yang, J.D. White, J.-H. Hsu, K.Y. Peng, S.A. Chen, and W. Fann, *Macromolecules* **2005**, *38*, 2966.
41. K.-Y. Peng, S.-A. Chen, W.-S. Fann, S.-H. Chen, and A.-C. Su, *J. Phys. Chem. B* **2005**, *109*, 9368.
42. E.J.W. List, C. Creely, G. Leising, N. Schulte, A.D. Schlüer, U. Scherf, K. Mülen, and W. Graupner, *Chem. Phys. Lett.* **2000**, *325*, 132.
43. J.G. Müller, U. Lemmer, G. Raschke, M. Anni, U. Scherf, J.M. Lupton, and J. Feldmann, *Phys. Rev. Lett.* **2003**, *91*, 267403.
44. G.P.D. Beljonne, C. Silva, E. Hennebicq, L.M. Herz, R.H. Friend, G.D. Scholes, S. Setayesh, K. Müllen, and J.L. Bredas, *Proc. Natl. Acad. Sci. USA* **2002**, *99*, 10982.
45. E. Hennebicq, G. Pourtois, G.D. Scholes, L.M. Herz, D.M. Russell, C. Silva, S. Setayesh, A.C. Grimsdale, K. Mullen, J.L. Bredas, and D. Beljonne, *J. Am. Chem. Soc.* **2005**, *127*, 4744.
46. L. Chen, D.W. McBranch, H.-L. Wang, R. Helgeson, F. Wudl, and D.G. Whitten, **1999**, *96*, 12287.
47. S. Kumaraswamy, T. Bergstedt, X. Shi, F. Rininsland, S. Kushon, W. Xia, K. Ley, K. Achyuthan, D. McBranch, and D. Whitten, *Proc. Natl. Acad. Sci. USA* **2004**, *101*, 7511.
48. F. Rininsland, W. Xia, S. Wittenburg, X. Shi, C. Stankewicz, K. Achyuthan, D. McBranch, and D. Whitten, *Proc. Natl. Acad. Sci. USA* **2004**, *101*, 15295.
49. F. Wang and G.C. Bazan, *J. Am. Chem. Soc.* **2006**, *128*, 15786.
50. B. Liu and G.C. Bazan, *J. Am. Chem. Soc.* **2006**, *128*, 1188.
51. B. Liu, S. Wang, G.C. Bazan, and A. Mikhailovsky, *J. Am. Chem. Soc.* **2003**, *125*, 13306.
52. B. Liu, S. Baudrey, L. Jaeger, and G.C. Bazan, *J. Am. Chem. Soc.* **2004**, *126*, 4076.
53. S. Wang, B.S. Gaylord, and G.C. Bazan, *J. Am. Chem. Soc.* **2004**, *126*, 5446.
54. C. Chi, A. Mikhailovsky, and G.C. Bazan, *J. Am. Chem. Soc.* **2007**, *129*, 11134.
55. E.S. Baker, J.W. Hong, B.S. Gaylord, G.C. Bazan, and M.T. Bowers, *J. Am. Chem. Soc.* **2006**, *128*, 8484.

56. C. Ego, D. Marsitzky, S. Becker, J. Zhang, A.C. Grimsdale, K. Mullen, J.D. MacKenzie, C. Silva, and R.H. Friend, *J. Am. Chem. Soc.* **2003**, *125*, 437.
57. J. Cabanillas-Gonzalez, A.M. Fox, J. Hill, and D.D.C. Bradley, *Chem. Mater.* **2004**, *16*, 4705.
58. L. Chen, S. Xu, D. McBranch, and D. Whitten, *J. Am. Chem. Soc.* **2000**, *122*, 9302.
59. F.J.M. Hoeben, P. Jonkheijm, E.W. Meijer, and A.P.H.J. Schenning, *Chem. Rev.* **2005**, *105*, 1491.
60. J. Jacob, S. Sax, T. Piok, E.J.W. List, A.C. Grimsdale, and K. Mullen, *J. Am. Chem. Soc.* **2004**, *126*, 6987.
61. S. Zheng, J. Shi, and R. Mateu, *Chem. Mater.* **2000**, *12*, 1814.
62. I.-W. Hwang, T. Kamada, T.K. Ahn, D.M. Ko, T. Nakamura, A. Tsuda, A. Osuka, and D. Kim, *J. Am. Chem. Soc.* **2004**, *126*, 16187.
63. Y. Nakamura, I. Hwang, N. Aratani, T.K. Ahn, D.M. Ko, A. Takagi, T. Kawai, T. Matsumoto, D. Kim, and A. Osuka, *J. Am. Chem. Soc.* **2005**, *127*, 236.
64. F. Hajjaj, Z.S. Yoon, M.-C. Yoon, J. Park, A. Satake, D. Kim, and Y. Kobuke, *J. Am. Chem. Soc.* **2006**, *128*, 4612.
65. M. Park, M.-C. Yoon, Z.S. Yoon, T. Hori, X. Peng, N. Aratani, J.-I. Hotta, H. Uji-i, M. Sliwa, J. Hofkens, A. Osuka, and D. Kim, *J. Am. Chem. Soc.* **2007**, *129*, 3539.
66. I.-W. Hwang, M. Park, T.K. Ahn, Z.S. Yoon, D.M. Ko, D. Kim, F. Ito, Y. Ishibashi, S.R. Khan, Y. Nagasawa, H. Miyasaka, C. Ikeda, R. Takahashi, K. Ogawa, A. Satake, and Y. Kobuke, *Chem. Eur. J.* **2005**, *11*, 3753.
67. M.-S. Choi, T. Aida, T. Yamazaki, and I. Yamazaki, *Chem. Eur. J.* **2002**, *8*, 2667.
68. D. Holten, D.F. Bocian, and J.S. Lindsey, *Acc. Chem. Res.* **2002**, *35*, 57.
69. B. Dietzek, W. Kiefer, J. Blumhoff, L. Bottcher, S. Rau, D. Walther, U. Uhlemann, M. Schmitt, and J. Popp, *Chem. Eur. J.* **2006**, *12*, 5105.